HHS Public Access

Author manuscript

Sci Transl Med. Author manuscript; available in PMC 2017 September 20.

Published in final edited form as:

Sci Transl Med. 2017 August 30; 9(405): . doi:10.1126/scitranslmed.aai8710.

Targeting the vascular and perivascular niches as a regenerative therapy for lung and liver fibrosis

Zhongwei Cao[1,2,*,†], **Tinghong Ye**[1,†], **Yue Sun**[1,†], **Gaili Ji**[1,†], **Koji Shido**[2], **Yutian Chen**[1], **Lin Luo**[1,3], **Feifei Na**[1,3], **Xiaoyan Li**[1], **Zhen Huang**[1], **Jane L. Ko**[4], **Vivek Mittal**[5], **Lina Qiao**[1], **Chong Chen**[1,3], **Fernando J. Martinez**[6], **Shahin Rafii**[2], and **Bi-Sen Ding**[1,2,*]

[1]Key Laboratory of Birth Defects and Related Diseases of Women and Children of MOE, State Key Laboratory of Biotherapy, West China Second University Hospital, Sichuan University, and Collaborative Innovation Center for Biotherapy, Chengdu, China

[2]Ansary Stem Cell Institute, Division of Regenerative Medicine, Department of Medicine, Weill Cornell Medicine, New York, NY 10065

[3]West China Hospital, Sichuan University, China

[4]Department of Biological Sciences, Seton Hall University, South Orange, NJ 07079

[5]Department of Cardiothoracic Surgery, Weill Cornell Medicine, New York, NY 10065

[6]Division of Pulmonary and Critical Care Medicine, Department of Medicine, Weill Cornell Medicine, New York, NY 10065

Abstract

The regenerative capacity of lung and liver is sometimes impaired by chronic or overwhelming injury. Orthotopic transplantation of parenchymal stem cells to damaged organs might reinstate their self-repair ability. However, parenchymal cell engraftment is frequently hampered by the microenvironment in diseased recipient organs. Here, we show that targeting both the vascular niche and perivascular fibroblasts establishes “hospitable soil” to foster incorporation of “seed”, in this case the engraftment of parenchymal cells in injured organs. Specifically, ectopic induction of endothelial cell (EC)-expressed paracrine/angiocrine hepatocyte growth factor (HGF) and inhibition of perivascular NADPH Oxidase 4 (NOX4) synergistically enabled reconstitution of mouse and human parenchymal cells in damaged organs. Reciprocally, genetic knockout of *Hgf* in mouse ECs ($Hgf^{i\Delta EC/i\Delta EC}$) aberrantly upregulated perivascular NOX4 during liver and lung regeneration. Dysregulated HGF and NOX4 pathways subverted the function of vascular and perivascular cells from an epithelially-inductive niche to a microenvironment that inhibited

*Correspondence addressed to Zhongwei Cao (zhc2007@med.cornell.edu); Bi-Sen Ding (bid2004@med.cornell.edu; dingbisen@scu.edu.cn).

†Contributed equally

Author Contributions: Z.C. conceived the project, performed the experiments, analyzed the results, and wrote the paper. T.Y., Y.S. G.J. designed and carried out the experiments, analyzed the data and edited the manuscript. K.S, Y.C, L.L, F.N., X.L., and Z.H. performed the experiments. J.L.K, V.M., L.Q., and C.C. analyzed the data. F.J.M commented on the study, and edited the manuscript. S.R. commented on the study. B.-S.D. designed and carried out the experiments, interpreted the results, and wrote the manuscript.

Competing interests: The authors have declared that no conflict of interest exists.

Data and materials availability: All materials are contained within manuscript and supplementary materials.

parenchymal reconstitution. Perivascular NOX4 induction in *Hgf*$^{i\Delta EC/i\Delta EC}$ mice recapitulated the phenotype of human and mouse fibrotic livers and lungs. Consequently, EC-directed HGF and NOX4 inhibitor GKT137831 stimulated regenerative integration of mouse and human parenchymal cells in chronically injured lung and liver. Our data suggest that targeting dysfunctional perivascular and vascular cells in diseased organs can bypass fibrosis and enable reparative cell engraftment to reinstate lung and liver regeneration.

Introduction

The self-repair capacity of liver and lung tissue is sometimes prohibited by overwhelming or persistent injury (1–19). Transplantation of parenchymal stem cells might aid in reinstating the regenerative ability (20–38), but efficient engraftment of parenchymal cells is handicapped by the prohibitive fibrotic microenvironment in diseased organs. Therefore, designing effective cell therapy strategies requires understanding how microenvironmental cues regulate parenchymal regeneration and fibrosis in the damaged lung and liver (39–47).

Surgical resection of liver or lung lobes by partial hepatectomy (PH) or pneumonectomy (PNX) triggers facultative regeneration without fibrosis (48–52). Liver and lung can also resolve fibrosis after acute injury (53–55). In contrast, chronic injury stimulates exuberant scar formation and fibrosis, leading to hepatic and pulmonary failure (56–63). How fibrosis is resolved after PH, PNX, or acute injury but triggered by chronic or overwhelming injury remains incompletely known (64–66). Since fibroblasts are the major cell type that produces matrix proteins during scar formation (59, 67–69), we hypothesized that modulating the interplay between perivascular fibroblasts and endothelial cells (ECs) might obviate fibrosis in the liver (2, 48, 49, 52) and lung (47, 70–73), forming an epithelially-inductive niche for parenchymal cell reconstitution and regeneration (74, 75).

Here we find that EC-expressed HGF prevents aberrant activation of NADPH Oxidase 4 (NOX4) (56, 76, 77) in perivascular fibroblasts after lung and liver injury. Induction of HGF and inhibition of NOX4 in damaged organs promotes the incorporation of regenerative parenchymal cells. We also devised a strategy to edit both vascular and perivascular cells by combining endothelial *Hgf* gene delivery with NOX4 inhibition. This dual niche-editing strategy enhanced functional reconstitution of mouse and human parenchymal cells, inducing fibrosis-free organ repair. Our data suggest that targeting vascular and perivascular cells in diseased organs might transform the prohibitive microenvironment to an epithelially-inductive niche that bypasses fibrosis and facilitates engraftment of regenerative progenitor cells.

Results

Repeated lung and liver injuries prohibit the incorporation of grafted parenchymal cells

We first tested the efficiency of parenchymal cell engraftment in both normal and injured mouse lung and liver. Non-injured and injured lungs were transplanted with type 2 alveolar epithelial cells (AEC2s), cells that contribute to lung epithelialization (14, 21, 24, 26) (Fig. 1A–B, fig. S1A), and livers were grafted with hepatocytes mediating hepatic reconstitution

(27, 33, 78) (Fig. 1C–D, fig. S1B). Lung injury was induced by intratracheal injection of bleomycin (Bleo) or hydrochloric acid (Acid) (46), and liver repair was triggered by intraperitoneal injection of carbon tetrachloride (CCl_4). To trace in vivo incorporation of transplanted parenchymal cells, AEC2-specific surfactant protein C-Cre^{ERT2} (Sftpc-Cre^{ERT2}) mice (14) and hepatocyte-specific Albumin-Cre mice were bred with TdTomato reporter mice. Isolated TdTomato^{+} AEC2 or hepatocytes were transplanted into mice via intratracheal or intrasplenic injection, respectively. We found that there was little parenchymal cell incorporation in the non-injured lung or liver (fig. S1A, B). In contrast, AEC2s and hepatocytes integrated into the injured lung or liver after the 3rd Bleo, Acid or CCl_4 injection (Fig. 1B, D).

Injured lung and liver either undergo fibrosis-free repair or develop fibrosis. A single Bleo or Acid injection triggers re-epithelialization in the injured lung without triggering fibrosis, but fibrosis starts to occur after repetitive injury (15). Similarly, CCl_4 injection stimulates hepatic regeneration after three injections, but the injured liver ceases to resolve fibrosis after multiple CCl_4 injections (16). Indeed, parenchymal cells failed to incorporate into the liver and lung after more than six injections of Bleo, Acid, or CCl_4 (Fig. 1B, D, fig. S1C), the stage at which injured liver and lung developed fibrosis (fig. S1D, E).

EC-produced HGF mitigates expression of pro-fibrotic NOX4 protein in perivascular fibroblasts

We then defined the microenvironment-derived cues that foster the incorporation of transplanted hepatocytes and AEC2s. Vascular ECs lining liver sinusoids or pulmonary capillaries were shown to elicit parenchymal regeneration (2, 16, 52, 79, 80). EC-produced HGF stimulates proliferation of parenchymal cells for organ repair (16, 48, 80–83). Thus, we tested whether endothelial HGF influences parenchymal cell engraftment. Mice expressing EC-specific VE-cadherin-driven Cre^{ERT2} (Cdh5-(PAC)-Cre^{ERT2}) (84) were bred with floxed *Hgf* mice (Fig. 1E). Mice were injected with tamoxifen to induce EC-specific ablation of *Hgf* (*Hgf*$^{i\Delta EC/i\Delta EC}$), and EC-specific *Hgf* heterozygous knockout (*Hgf*$^{i\Delta EC/+}$) mice were used as controls (fig. S2A).

Lung and liver repair were analyzed in *Hgf*$^{i\Delta EC/i\Delta EC}$ and control mice after the 3rd Bleo or CCl_4 injection (Fig. 1E). Compared with control mice, there was increased lethality in *Hgf*$^{i\Delta EC/i\Delta EC}$ mice after liver or lung injury, which was associated with elevated tissue destruction and increased fibrosis in *Hgf*$^{i\Delta EC/i\Delta EC}$ liver and lung (Fig. 1F–I, fig. S2B–C). Consequently, incorporation of transplanted parenchymal cells was suppressed in the injured *Hgf*$^{i\Delta EC/i\Delta EC}$ lung or liver, as compared with than that of controls (Fig. 1J, K). Hence, EC-produced HGF promotes organ repair, resolves fibrosis, and facilitates the engraftment of parenchymal cells in the injured lung and liver.

Hgf$^{i\Delta EC/i\Delta EC}$ mice were then characterized in another liver regeneration model induced by PH. Qualitative immunostaining analysis suggested that hepatocyte proliferation after PH was lower in *Hgf*$^{i\Delta EC/i\Delta EC}$ mice than controls (Fig. 2A), and collagen deposition and cell apoptosis were elevated in the liver of hepatectomized *Hgf*$^{i\Delta EC/i\Delta EC}$ mice compared to controls (Fig. 2B–C). Immunostaining and ELISA analysis of Malondialdehyde (MDA) revealed markedly higher peroxide formation in *Hgf*$^{i\Delta EC/i\Delta EC}$ mouse liver after PH (Fig.

2D–E). Hepatectomized *Hgf*$^{i\Delta EC/i\Delta EC}$ mice also exhibited increased lethality and liver damage than controls, as evidenced by higher serum bilirubin concentration (fig. S2D–E). Thus, HGF expressed by ECs stimulates parenchymal cell expansion and resolves fibrosis during PH-induced liver regeneration.

Increased fibrosis and oxidative damage in *Hgf*$^{i\Delta EC/i\Delta EC}$ mice led us to identify the influence of endothelial HGF on perivascular fibroblasts. HGF was shown to attenuate the expression of the NOX family of proteins that regulate redox balance (85), and elevated NOX activity after injury stimulates fibrosis (56, 76). Indeed, after PH and three CCl_4 injections, NOX4 expression was increased in the liver of *Hgf*$^{i\Delta EC/i\Delta EC}$ mice than that of controls (Fig. 2F–H). Furthermore, NOX4 protein was found to be preferentially distributed in perivascular fibroblasts of hepatectomized *Hgf*$^{i\Delta EC/i\Delta EC}$ mice (Fig. 2I). As such, development of fibrosis in *Hgf*$^{i\Delta EC/i\Delta EC}$ mice in liver regeneration is associated with NOX4 induction in perivascular fibroblasts.

To establish the correlation between endothelial HGF and perivascular NOX4 in fibrogenesis, we adopted a liver-specific gene transduction system (86). Bolus injection of a large volume of gene material via tail vein caused gene transduction in the mouse liver (fig. S2F). This system allowed us to study the contribution of Nox4 to liver regeneration in *Hgf*$^{i\Delta EC/i\Delta EC}$ mice. Silencing Nox4 expression in hepatectomized or CCl_4-injured *Hgf*$^{i\Delta EC/i\Delta EC}$ mice promoted liver regeneration and blocked fibrosis (fig. S2G–J). Thus, endothelial HGF stimulates fibrosis-free liver repair at least partially by suppressing NOX4 upregulation in perivascular fibroblasts.

We then sought to define the hepatic-protective effect of endothelial HGF in a liver cholestasis model, bile duct ligation (BDL). The common bile duct was ligated and resected to induce biliary epithelial injury. BDL caused perivascular NOX4 protein upregulation and stimulated qualitatively higher degrees of cell apoptosis, peroxide formation, and collagen deposition in *Hgf*$^{i\Delta EC/i\Delta EC}$ livers than controls (Fig. 2J–O, fig. S2K). As such, loss of HGF expression in EC might stimulate perivascular fibroblast activation in cirrhotic liver.

The clinical relevance of the HGF-NOX4 axis was investigated in samples of liver from human cirrhotic patients. Immunostaining of NOX4 and desmin showed that the extent of fibrosis positively correlated with NOX4 protein expression in the cirrhotic livers (Fig. 3A). NOX4 was qualitatively upregulated in perivascular desmin$^+$ fibroblasts adjacent to VE-cadherin$^+$ ECs (Fig. 3B–D, fig. S3A–H). Thus, NOX4 upregulation in perivascular fibroblasts of injured *Hgf*$^{i\Delta EC/i\Delta EC}$ liver was reminiscent of aberrant expression of perivascular NOX4 in human cirrhotic livers.

Since tumor growth factor-β (TGF-β) stimulates NOX4 expression in fibroblasts (56, 76), we investigated whether endothelial HGF influences NOX4 expression in fibroblasts in the presence of TGF-β. Human and mouse hepatic stellate cells were treated with TGF-β with or without HGF. HGF ameliorated NOX4 expression and activity in human and mouse stellate cells after TGF-β stimulation (Fig. 3E–F, fig. S3I–J). An endothelial-stellate cell co-culture system was used to explore the crosstalk between endothelial HGF and fibroblast NOX4 (Fig. 3G). NOX4 protein expression was lower in stellate cells cultured with ECs

overexpressing HGF (EC^{HGF}) than those with control ECs with scrambled sequence (EC^{Srb}) (Fig. 3H–J).

Targeting vascular and perivascular cells improves the engraftment of mouse and human parenchymal cells in fibrotic livers

Building on the finding that endothelial HGF promotes liver regeneration, we postulated that ectopic expression of HGF in the liver ECs (87–89) could enhance hepatocyte engraftment in the injured liver. To test this hypothesis, we adopted a pseudotyped lentivirus system that conjugates with immunoglobulin antibody at the viral surface (90). Coupling of pseudotyped lentivirus with antibody recognizing EC antigen CD31 allows for gene transfer in ECs (15). Mouse CD31 antibody (Mec13.3) was conjugated with virus encoding green fluorescent protein (*Gfp*), scrambled sequence (*Srb*), or *Hgf*, resulting in Mec13-*Gfp*, Mec13-*Srb*, and Mec13-*Hgf* viruses.

Intra-splenic injection was employed to localize Mec13-virus in the hepatic vascular bed. Compared to control (Mec13-*Srb)*, Mec13-*Hgf* attenuated perivascular NOX4 expression in BDL-injured liver (Fig. 4A–B, fig. S4A). Subsequently, we tested whether combining Mec13-*Hgf* with NOX4 inhibitor GKT137831 (GKT) would more efficiently provoke regeneration in the injured liver. GKT was administered to injured mice together with Mec13-*Hgf* (Mec13-*Hgf* + GKT). Mec13-*Hgf* + GKT substantially lowered peroxide formation and hydroxyproline amounts after BDL, more than any other tested treatments (Fig. 4C–E). Moreover, Mec13-*Hgf* + GKT efficiently promoted the incorporation of grafted mouse hepatocytes (Fig. 4F) and induced the most efficacious hepatic repair in all tested approaches (Fig. 4G–I).

We then tested how dual niche-editing influences reconstitution of human hepatocytes (Fig. 5A). Immunodeficient NOD-Prkdc^{em26Cd52}Il2rg^{em26Cd22}/Nju (NCG) mice treated with Mec13-*Srb*, Mec13-*Hgf*, GKT, or Mec13-*Hgf* + GKT after BDL. Human hepatocytes were transplanted into the injured mice via intrasplenic injection. Mec13-*Hgf* + GKT enhanced the incorporation of GFP-labeled human hepatocytes in the damaged liver, and these grafted hepatocytes maintained the expression of hepatocyte marker cholesterol 7alpha-hydroxylase (CYP7A1) (Fig. 5B). NCG mice treated with Mec13-*Hgf* + GKT + human hepatocytes showed reduced cell death in the liver, regenerated hepatic architecture and function, and higher serum human albumin concentration than all other test groups (Fig. 5C–G, fig. S4B). Therefore, dual editing of vascular and perivascular cells bypasses fibrosis to enable the engraftment of mouse and human parenchymal cells, promoting hepatic regeneration (Fig. 5H).

Endothelial HGF suppresses pro-fibrotic expression of NOX4 in perivascular lung fibroblasts

To explore the generality of the observed regenerative effect of endothelial HGF, we tested *Hgf*$^{i\Delta EC/i\Delta EC}$ mice in a lung alveolar regeneration model triggered by PNX. PNX stimulates functional growth of the intact right lung lobe after surgical resection of the left lung lobe (Fig. 6A). Compared to the controls, *Hgf*$^{i\Delta EC/i\Delta EC}$ mice had increased peroxide formation and NOX4 protein expression after PNX (Fig. 6B–C), which was accompanied by inhibited

restoration of lung mass and function, and qualitatively elevated cell apoptosis (fig. S5A–D). Notably, NOX4 was qualitatively upregulated in perivascular fibroblasts in pneumonectomized *Hgf*$^{i\Delta EC/i\Delta EC}$ mice (Fig. 6D). Hence, endothelial HGF has a similarly important role in driving lung alveolar regeneration and obviating fibrosis after PNX.

To investigate the relationship between endothelial HGF and NOX4 in lung regeneration, we silenced *Nox4* in injured mouse lungs (56). Nox4 shRNA was administered intratracheally into the pneumonectomized *Hgf*$^{i\Delta EC/i\Delta EC}$ mice (fig. S5E). This method blocked the upregulation of NOX4 in perivascular fibroblasts, prevented fibrosis, and restored alveolar function in pneumonectomized *Hgf*$^{i\Delta EC/i\Delta EC}$ lungs (fig. S5F–I). Of note, HGF blocked upregulation of NOX4 protein in cultured human and mouse lung fibroblasts after TGF-β treatment (Fig. 6E–F, fig. S6A–B), and incubating human lung fibroblasts with EC^{HGF} abrogated NOX4 protein induction by TGF-β (Fig. 6G–H, fig. S6C). The degree of NOX4 upregulation in perivascular fibroblasts correlated with fibrosis grade in human fibrotic lung tissue samples (Fig. 6I), and perivascular NOX4 induction in *Hgf*$^{i\Delta EC/i\Delta EC}$ mouse lungs after PNX recapitulated NOX4 expression in perivascular fibroblasts of human fibrotic lungs (Fig. 6J–L, fig. S6D–K). Therefore, endothelial HGF suppresses expression of NOX4 in perivascular lung fibroblasts, which may contribute to fibrogenesis in diseased human lungs.

Targeting dysfunctional vascular and perivascular cells enhances engraftment of AEC2s in fibrotic lungs

We investigated the therapeutic effect of Mec13-*Hgf* and GKT after repeated Bleo or Acid injections using mouse models. Jugular vein injection of Mec13-*Hgf* (15) in mice inhibited NOX4 upregulation in injured lung fibroblasts (Fig. 7A, B). Qualitative Sirius red staining implicated that Mec13-*Hgf* + GKT reduced fibrosis in the injured lungs (Fig. 7C). Moreover, Mec13-*Hgf* + GKT enhanced incorporation of AEC2s in damaged lungs, which stimulated lung regeneration more efficiently than any other treatments (Fig. 7D–F). These data suggest that editing dysfunctional vascular and perivascular cells can subvert an epithelially-prohibitive microenvironment to an epithelially-active niche, enabling regenerative therapy for fibrosis (fig. S7A).

We also tested the efficacy of Mec13-*Hgf* + GKT on promoting reconstitution of human AEC2s. NCG mice were subjected to either Bleo or Acid injury and transplanted with GFP-labeled human AEC2s after Mec13-*Srb*, Mec13-*Hgf*, GKT, or Mec13-*Hgf* + GKT treatment (Fig. 8A). Mec13-*Hgf* + GKT efficiently promoted human AEC2 incorporation in the recipient mouse lungs (Fig. 8B). This engraftment was accompanied by blunted cell death, restored alveolar architecture, and recovered gas exchange function (Fig. 8C–E, fig. S7B).

Discussion

The microenvironment of recipient organ, the “soil”, can regulate the efficiency of cell engraftment. Establishing an epithelially inductive microenvironment in diseased organs might facilitate the engraftment of regenerative parenchymal cells. In this study, we find that vascular and perivascular niche cells jointly regulate the incorporation of transplanted alveolar progenitor cell or hepatocyte in damaged organs. Parenchymal cell incorporation in injured lungs and livers requires expression of HGF in the endothelial niche and suppression

of perivascular NOX4 activity. Moreover, incorporated parenchymal cells synergize with targeted niches to stimulate the most efficacious organ repair. Thus, reinstating self-repair capacity of diseased lung and liver might require the co-operation between the pro-regenerative microenvironment and grafted parenchymal stem/progenitor cells.

Fibrosis in injured organs might hamper engraftment of parenchymal cells. Therefore, understanding of how fibrosis is resolved during organ regeneration is helpful for devising cellular therapy for various diseases (1, 5). HGF has an important role in promoting parenchymal cell expansion (83, 91–94). Here we found that EC-expressed HGF contributes to resolving lung and liver fibrosis, which is at least partially mediated by suppressing NOX4 expression in perivascular fibroblasts. In PH and PNX models that induce parenchymal regeneration without fibrosis, deletion of *Hgf* in mouse EC blocked regeneration and caused fibrosis. Reciprocally, in mouse liver and lung fibrosis models, ectopic expression of *Hgf* in EC prevented activation of perivascular fibroblast and suppressed fibrosis. These genetic model-based *in vivo* and *in vitro* cultivation data implicate that in addition to stimulating parenchymal reconstitution, endothelial HGF also serves as a key molecule to prevent fibrosis.

Therapeutically, NOX4 inhibition synergized with endothelial HGF induction to stimulate efficacious parenchymal reconstitution and regeneration. This synergistic effect may be due to several layers of mechanisms. First, reduced NOX4 in perivascular cells by endothelial HGF might require less NOX4 inhibitor to reach sufficient inhibition. Second, reducing oxidative stress in the damaged organs by NOX4 inhibitor may promote production or activation of HGF from the vascular niche. The additive effects by endothelial HGF and NOX4 inhibition might also rely on operative mechanisms independent of the HGF-NOX4 axis. Endothelial HGF can exert various regenerative functions (91–94), and this dual editing approach might utilize both NOX4-dependent and NOX4-independnet mechanisms. NOX4 inhibition prevents parenchymal cell death after injury (95), offering hepatogenic or alveologenic effects that extend beyond HGF signaling. As such, our dual editing approach might exploit various functions of HGF and NOX4 that are independent of the HGF-NOX4 axis.

HGF expression triggered in the vascular niche after parenchymal injury may act as a protective response. The vast surface area of hepatic or pulmonary microvasculature is ideal to deploy enormous amounts of paracrine growth factors within a short time period (2, 75, 96–98). Several endothelial receptors were demonstrated to mediate HGF upregulation in ECs, including VEGFR1 (48), VEGFR2 (80), and CXCR7 (16). Conceivably, these endothelial receptors sense tissue mass loss or chemical injury to trigger HGF expression. Loss of these pathways might not only impair regeneration but also cause fibrosis. It was shown before that activation of Smad2/3 blocks HGF transcription in keratinocytes (99). Whether the TGF/Smad pathway mediates the subversion of epithelially-inductive vascular niche function during parenchymal repair can be explored in the future.

The translational value of the dual niche-editing system could be improved through alternate gene transfer methods or coupling to different inhibitors or therapeutics. Pseudotyped lentivirus accomplishes EC-selective gene transfer at the expense of low efficiency; a

therapeutically applicable EC gene editing approach might require a clinically tested gene transfer system with higher efficiency. Engineered Adeno-associated virus (AAV) can be chemically conjugated with an endothelial targeting moiety via process such as biotin-avidin interaction (87, 89). Administration of EC-targeted AAV can potentially offer more efficacious and safer vascular gene editing in fibrotic organs. Other therapeutics can be exploited to target the dysfunctional perivascular niche in conjugation with NOX4 inhibitor.

Taken together, we show that vascular and perivascular cells jointly influence the engraftment of parenchymal progenitor cells in the inured lungs and livers. Implementing cell transplantation with niche editing efficiently induces organ regeneration. Our proof-of-principle evidence may help develop cell therapy approaches to enable fibrosis-free repair in various organs.

Materials and Methods

Study Design

We combined vascular *Hgf* gene expression with NOX4 inhibition via GKT137831 to edit the vascular and perivascular niches in fibrotic lung and liver. The contribution of vascular and perivascular niches were demonstrated by suppressed parenchymal cell engraftment in host mice lacking endothelial HGF and overexpressing perivascular NOX4. The role of endothelial HGF in promoting parenchymal regeneration and bypassing fibrosis in liver and lung was established using *1*) EC-specific knockout ($Hgf^{i\Delta EC/i\Delta EC}$) mice and *2*) complementary lung and liver regeneration and repair models. Both AEC2s and hepatocytes were grafted into recipient mice after treatment with EC-targeted *Hgf*, GKT137831, or combination therapy. We analyzed the extent of incorporation of transplanted mouse and human parenchymal cells in the recipient mice, and tested the efficacy of functional organ repair in liver and lung injury models. Investigators who performed mouse experiments and who analyzed the pattern and extent of cell distribution and tissue pathology were randomly assigned with animal or human samples. Investigators were blinded to the phenotypes of samples from different groups. For quantitative experiments consisting of $n < 20$ animals per group, individual level data are shown in table S1.

Genetic mouse models

The AEC2-specific Sftpc-Cre^{ERT2} mouse line was kindly provided by Dr. Brigid Hogan at Duke University, and hepatocyte-specific Albumin-Cre mouse and ROSA26-TdTomato reporter mouse expressing TdTomato after floxed stop codon were purchased from the Jackson Laboratories. Sftpc-Cre^{ERT2} and Albumin-Cre mice were bred with ROSA26-TdTomato mice, and Sftpc-Cre^{ERT2} expression in the offspring mouse was induced by 6 consecutive intraperitoneal injections of 100 mg/kg tamoxifen (Sigma-Aldrich). Expression of Cre induced excision of the stop codon preceding TdTomato and triggered expression of red fluorescent protein in AEC2s and hepatocytes. Floxed *Hgf* mice were obtained from mutant mouse regional resource centers (No 000423). Mice expressing EC-specific Cdh5-(PAC)-Cre^{ERT2} (84) were provided by Dr. Ralf Adams. This mouse line was crossed with floxed *Hgf* mice to generate $Hgf^{i\Delta EC/i\Delta EC}$ mice and control $Hgf^{i\Delta EC/+}$ mice after treatment of tamoxifen at a dose of 150 mg/kg for 6 days, and interrupted for 3 days after the third

dose. Deletion of target genes in ECs was corroborated by quantitative polymerase chain reaction (PCR). Six to ten weeks old sex and weight matched *Hgf*$^{i\Delta EC/i\Delta EC}$ and *Hgf*$^{i\Delta EC/+}$ mice and male *WT* mice were used for mouse PH, PNX and liver and lung injury models. Six to ten weeks old immunodeficient NCG mice from Nanjing Biomedical Research Institute of Nanjing University were used for transplantation of human hepatocytes and AEC2s. All animal experiments were carried out by protocols approved by the Institutional Animal Care and Use Committee at Sichuan University and Weill Cornell Medicine.

Liver and lung injury models

Injections of CCl_4 were used to induce liver injury as previously described (16). CCl_4 was diluted in olive oil (Sigma-Aldrich) to yield a concentration of 40% (0.64 mg/ml) and intraperitoneally injected to mice at a dose of 1.6 g/kg. Mice were subjected to BDL to induce cirrhotic liver injury (16). To perform BDL, mice were anesthetized with a cocktail of ketamine (100 mg/kg) and xylazine (10 mg/kg). Ketamine and xylazine were provided by approved veterinary service at Weill Cornell Medicine. Repetitive intratracheal bleomycin or hydrochloric acid injection models were used to induce lung injury (100). At the described time points, oxygen tension in arterial blood of treated mice was measured using I-Stat (Abbott Laboratories).

Transplantation of mouse and human parenchymal cells

AEC2s and hepatocytes expressing TdTomato were isolated as described (21, 51, 80). To isolate AEC2s, the mouse lungs were removed and digested in cocktail solution containing 2 mg/ml collagenase A and 1 mg/ml Dispase (Roche Life Science) in Hanks' Balanced Salted Solution (HBSS). 1 ml digestion solution was directly instilled via the trachea and used to perfuse via pulmonary artery to accelerate the digestion process. Perfused mouse lungs were removed from the chest cavity to endothelial cell growth medium (Sigma-Aldrich), minced, and disrupted. Lungs were then suspended in 2.5 ml/100mg digestion cocktail at 37 °C for 15 min. Digested lungs were filtered through a 40 μm nylon mesh (cell strainer) and centrifuged. Cell suspension was centrifuged via Percoll gradient. AEC2 band was harvested, and TdTomato$^+$ AEC2s were sorted by flow cytometry. Human AEC2s were purchased from iCell Bioscience Inc.

For mouse AEC2 transplantation, 3 million isolated mouse AEC2s were infused into mouse lungs via trachea 3 days after the 3rd or 6th Bleo or Acid treatment. Mice were also treated with Mec13-*Srb*, Mec13-*Hgf*, GKT, or Mec13-*Hgf* + GKT after the 3rd Bleo or Acid, and 3 million of mouse AEC2s were transplanted after 5th Bleo or 6th Acid. For human AEC2 transplantation, ten million human AEC2s were labeled with GFP and transplanted into immunodeficient NCG mice after indicated treatments. Recipient mice were sacrificed ten days after transplantation to determine the incorporation of transplanted cells in the injured lungs. Blood oxygen tension was analyzed 20 days after last Bleo or Acid injury.

Hepatocytes were purified as described via a two-step perfusion and digestion procedure (51, 80). Human hepatocytes were obtained from BioreclamationIVT. For mouse hepatocyte transplantation, 2.5 million isolated mouse hepatocytes were transplanted to the injured mouse liver via intrasplenic injection (80) three days after the 3rd or 8th injection of CCl_4.

Intrasplenic injection was also performed as described (80). Ten million human hepatocytes were transplanted into NCG mice at day 10 after BDL injury. Recipient mice were sacrificed at day 21 after BDL to assess the extent of hepatocyte incorporation in the injured liver.

Mouse liver and lung injury models

A mouse PH model was used to induce liver regeneration (80). Left lung PNX model and measurement of alveolar regeneration (79, 98) and lung injury (15) were adapted. Animal experiment procedures are described in supplementary methods. Liver and lung fibrotic responses were determined at the indicated time after injection of Bleo, Acid, CCl_4, or BDL. Collagen distribution was assessed by Sirius red staining (15). Hydroxyproline amount was quantified in the liver and lung to determine the extent of fibrosis (15, 55). To measure peroxide formation in the tissue, immunostaining and ELISA of MDA were performed using antibody against MDA (Abcam) and a lipid peroxidation assay kit (Abcam). Generation of H_2O_2 in cultured stellate cells and lung fibroblasts were performed as described (76).

Culture of hepatic stellate cell and lung fibroblast

For co-culture experiments with human ECs, 200 ul matrigel (BD Biosciences) was incubated in 24 well plate, and fluorescently labeled human stellate cell LX-2 or lung fibroblasts and mCherry-labeled ECs were seeded at 1 to 1 ratio on matrigel (BD biosciences). Formation of 3 dimensional vascular tubes was imaged by fluorescent microscope. Human stellate cell line LX-2 was generously provided by Dr. Scott Friedman (Mount Sinai Hospital), and mouse hepatic stellate cell was obtained from ScienceCell Research Laboratories. Human and mouse lung fibroblasts were purchased from Science Cell Inc. Human ECs were obtained from Angiocrine Bioscience. Cultured stellate and fibroblast cells were treated with 20 ng/ml recombinant TGF-β and 40 ng/ml HGF (PeproTech Inc.) and retrieved for NOX4 protein analysis by Western blot.

NOX4 inhibitor GKT137831 and EC-specific delivery of *Hgf*

Pseudotyped lentiviral particles containing *Hgf* were conjugated with Mec13.3 antibody to induce HGF expression in endothelial cell (Mec13-*Hgf*). Lentivirus containing *Srb* construct was similarly processed with Mec13.3 as a control group (Mec13-*Srb*). After the third Bleo, Acid injection or BDL, six to eight weeks old mice were subjected to Mec13-*Hgf* or Mec13-*Srb* every three days at a dose of 75 μg p24 capsid protein. The effect of GKT137831 was tested in lung and liver fibrosis models. GKT137831 was dissolved in an aqueous solution (0.5% carboxymethylcellulose and 0.25% Tween 20). 10 mg/kg GKT137831 was given to mice twice weekly by oral gavage (started together with Mec13-*Hgf*) (56, 76). The effect of combination treatment was compared with vehicle, Mec13-*Hgf*, or GKT137831 alone.

Immunostaining and histological analysis of mouse and human cryosections

Mouse liver and lung tissues were harvested for histological analysis (16, 80). Human sample sources are described in supplementary material. For immunofluorescent microscopy, the liver sections (10 μm) were blocked (5% donkey serum/0.3% Triton X-100) and incubated in primary antibodies: anti-VE-cadherin polyclonal antibody (pAb, 2 μg/ml, R&D Systems), anti-NOX4 (pAb, 5 μg/ml, Abcam), anti-MDA antibody (5 μg/ml, Ab6463,

Abcam), and anti-desmin (pAb, 2 μg/ml, Abcam). After incubation in fluorophore-conjugated secondary antibodies (2.5 μg/ml, Jackson ImmunoResearch), sections were counterstained with DAPI (Invitrogen). For each animal, five sections were analyzed for each animal.

Image acquisition and analysis

Histology analysis and Sirius red staining of liver or lung sections were captured with Olympus BX51 microscope (Olympus America, NY). Densitometry analysis of Western blot image was performed with ImageJ software using calibrated standard curve of optical density, and fluorescent images were recorded on AxioVert LSM710 confocal microscope (Zeiss).

Statistical analysis

All data were presented as the mean ± standard error of mean (S.E.M). For statistical analysis of experiments where there are more than two treated groups, one-way analysis of variance (ANOVA) was performed, followed by Tukey's test as post hoc analysis. Comparison of statistical difference between two experimental groups was determined by two tailed t-test.

Supplementary Material

Refer to Web version on PubMed Central for supplementary material.

Acknowledgments

We are grateful to Dr. Scott L. Friedman (Mount Sinai Hospital, NY) for kindly providing human hepatic stellate cell LX-2. We want to thank Dr. Irvin S.Y. Chen (UCLA, CA) for offering pseudotype virus vector. We are indebted to Dr. Ralf H. Adams (Max Planck Institute, Germany) and Dr. Brigid L.M. Hogan (Duke University, NC) for EC-specific Cdh5-(PAC)-Cre^{ERT2} mice and AEC2-specific Sftpc-Cre^{ERT2} mouse line.

Funding: This work was supported by National Scientist Development Grant from the American Heart Association (12SDG1213004), National Heart, Lung, and Blood Institute (R01HL097797, R01HL119872, R01HL130826), National Natural Science Foundation of China (91639117), and National Key Research and Development Program focused on Stem Cell and Translational Research (2016YFA0101600). S.R. is also supported by the Empire State Stem Cell Board and New York State Department of Health grants (C024180, C026438, C026878, C028117).

References

1. Friedman SL, Sheppard D, Duffield JS, Violette S. Therapy for fibrotic diseases: nearing the starting line. Science translational medicine. 2013; 5:167sr161. published online EpubJan 9. doi: 10.1126/scitranslmed.3004700
2. Hu J, Srivastava K, Wieland M, Runge A, Mogler C, Besemfelder E, Terhardt D, Vogel MJ, Cao L, Korn C, Bartels S, Thomas M, Augustin HG. Endothelial cell-derived angiopoietin-2 controls liver regeneration as a spatiotemporal rheostat. Science. 2014; 343:416–419. published online EpubJan 24. [PubMed: 24458641]
3. Kotton DN, Morrisey EE. Lung regeneration: mechanisms, applications and emerging stem cell populations. Nature medicine. 2014; 20:822–832. published online EpubAug. DOI: 10.1038/nm.3642
4. Wynn TA, Ramalingam TR. Mechanisms of fibrosis: therapeutic translation for fibrotic disease. Nature medicine. 2012; 18:1028–1040. published online EpubJul.

5. Thannickal VJ, Zhou Y, Gaggar A, Duncan SR. Fibrosis: ultimate and proximate causes. The Journal of clinical investigation. 2014; 124:4673–4677. published online EpubNov. DOI: 10.1172/JCI74368 [PubMed: 25365073]
6. Raghu G, Anstrom KJ, King TE Jr, Lasky JA, Martinez FJ. N. Idiopathic Pulmonary Fibrosis Clinical Research. Prednisone, azathioprine, and N-acetylcysteine for pulmonary fibrosis. The New England journal of medicine. 2012; 366:1968–1977. published online EpubMay 24. DOI: 10.1056/NEJMoa1113354 [PubMed: 22607134]
7. Hogan BL, Barkauskas CE, Chapman HA, Epstein JA, Jain R, Hsia CC, Niklason L, Calle E, Le A, Randell SH, Rock J, Snitow M, Krummel M, Stripp BR, Vu T, White ES, Whitsett JA, Morrisey EE. Repair and regeneration of the respiratory system: complexity, plasticity, and mechanisms of lung stem cell function. Cell stem cell. 2014; 15:123–138. published online EpubAug 07. DOI: 10.1016/j.stem.2014.07.012 [PubMed: 25105578]
8. Mehal WZ, Iredale J, Friedman SL. Scraping fibrosis: expressway to the core of fibrosis. Nature medicine. 2011; 17:552–553. published online EpubMay.
9. Eming SA, Martin P, Tomic-Canic M. Wound repair and regeneration: mechanisms, signaling, and translation. Science translational medicine. 2014; 6:265sr266. published online EpubDec 3. doi: 10.1126/scitranslmed.3009337
10. Loeys BL, Gerber EE, Riegert-Johnson D, Iqbal S, Whiteman P, McConnell V, Chillakuri CR, Macaya D, Coucke PJ, De Paepe A, Judge DP, Wigley F, Davis EC, Mardon HJ, Handford P, Keene DR, Sakai LY, Dietz HC. Mutations in fibrillin-1 cause congenital scleroderma: stiff skin syndrome. Science translational medicine. 2010; 2:23ra20. published online EpubMar 17. doi: 10.1126/scitranslmed.3000488
11. Reed NI, Jo H, Chen C, Tsujino K, Arnold TD, DeGrado WF, Sheppard D. The alphavbeta1 integrin plays a critical in vivo role in tissue fibrosis. Science translational medicine. 2015; 7:288ra279. published online EpubMay 20. doi: 10.1126/scitranslmed.aaa5094
12. Bataller R, Brenner DA. Liver fibrosis. The Journal of clinical investigation. 2005; 115:209–218. published online EpubFeb. [PubMed: 15690074]
13. Xu Y, Mizuno T, Sridharan A, Du Y, Guo M, Tang J, Wikenheiser-Brokamp KA, Perl AT, Funari VA, Gokey JJ, Stripp BR, Whitsett JA. Single-cell RNA sequencing identifies diverse roles of epithelial cells in idiopathic pulmonary fibrosis. JCI insight. 2016; 1:e90558. published online EpubDec 08. doi: 10.1172/jci.insight.90558 [PubMed: 27942595]
14. Rock JR, Barkauskas CE, Cronce MJ, Xue Y, Harris JR, Liang J, Noble PW, Hogan BL. Multiple stromal populations contribute to pulmonary fibrosis without evidence for epithelial to mesenchymal transition. Proceedings of the National Academy of Sciences of the United States of America. 2011; 108:E1475–1483. published online EpubDec 27. [PubMed: 22123957]
15. Cao Z, Lis R, Ginsberg M, Chavez D, Shido K, Rabbany SY, Fong GH, Sakmar TP, Rafii S, Ding BS. Targeting of the pulmonary capillary vascular niche promotes lung alveolar repair and ameliorates fibrosis. Nature medicine. 2016; 22:154–162. published online EpubFeb. DOI: 10.1038/nm.4035
16. Ding BS, Cao Z, Lis R, Nolan DJ, Guo P, Simons M, Penfold ME, Shido K, Rabbany SY, Rafii S. Divergent angiocrine signals from vascular niche balance liver regeneration and fibrosis. Nature. 2014; 505:97–102. published online EpubJan 2. DOI: 10.1038/nature12681 [PubMed: 24256728]
17. Gurtner GC, Werner S, Barrandon Y, Longaker MT. Wound repair and regeneration. Nature. 2008; 453:314–321. published online EpubMay 15. [PubMed: 18480812]
18. Zhao J, Zhang Z, Luan Y, Zou Z, Sun Y, Li Y, Jin L, Zhou C, Fu J, Gao B, Fu Y, Wang FS. Pathological functions of interleukin-22 in chronic liver inflammation and fibrosis with hepatitis B virus infection by promoting T helper 17 cell recruitment. Hepatology (Baltimore, Md. 2014; 59:1331–1342. published online EpubApr. DOI: 10.1002/hep.26916
19. Manavski Y, Abel T, Hu J, Kleinlutzum D, Buchholz CJ, Belz C, Augustin HG, Boon RA, Dimmeler S. Endothelial transcription factor KLF2 negatively regulates liver regeneration via induction of activin A. Proceedings of the National Academy of Sciences of the United States of America. 2017; 114:3993–3998. published online EpubApr 11. DOI: 10.1073/pnas.1613392114 [PubMed: 28348240]
20. Vaughan AE, Brumwell AN, Xi Y, Gotts JE, Brownfield DG, Treutlein B, Tan K, Tan V, Liu FC, Looney MR, Matthay MA, Rock JR, Chapman HA. Lineage-negative progenitors mobilize to

regenerate lung epithelium after major injury. Nature. 2015; 517:621–625. published online EpubJan 29. DOI: 10.1038/nature14112 [PubMed: 25533958]

21. Desai TJ, Brownfield DG, Krasnow MA. Alveolar progenitor and stem cells in lung development, renewal and cancer. Nature. 2014 published online EpubFeb 5.
22. Zuo W, Zhang T, Wu DZ, Guan SP, Liew AA, Yamamoto Y, Wang X, Lim SJ, Vincent M, Lessard M, Crum CP, Xian W, McKeon F. p63(+)Krt5(+) distal airway stem cells are essential for lung regeneration. Nature. 2015; 517:616–620. published online EpubJan 29. DOI: 10.1038/nature13903 [PubMed: 25383540]
23. Tata PR, Mou H, Pardo-Saganta A, Zhao R, Prabhu M, Law BM, Vinarsky V, Cho JL, Breton S, Sahay A, Medoff BD, Rajagopal J. Dedifferentiation of committed epithelial cells into stem cells in vivo. Nature. 2013; 503:218–223. published online EpubNov 14. [PubMed: 24196716]
24. Liang J, Zhang Y, Xie T, Liu N, Chen H, Geng Y, Kurkciyan A, Mena JM, Stripp BR, Jiang D, Noble PW. Hyaluronan and TLR4 promote surfactant-protein-C-positive alveolar progenitor cell renewal and prevent severe pulmonary fibrosis in mice. Nature medicine. 2016; 22:1285–1293. published online EpubNov. DOI: 10.1038/nm.4192
25. Huang SX, Islam MN, O'Neill J, Hu Z, Yang YG, Chen YW, Mumau M, Green MD, Vunjak-Novakovic G, Bhattacharya J, Snoeck HW. Efficient generation of lung and airway epithelial cells from human pluripotent stem cells. Nature biotechnology. 2014; 32:84–91. published online EpubJan. DOI: 10.1038/nbt.2754
26. Barkauskas CE, Cronce MJ, Rackley CR, Bowie EJ, Keene DR, Stripp BR, Randell SH, Noble PW, Hogan BL. Type 2 alveolar cells are stem cells in adult lung. The Journal of clinical investigation. 2013; 123:3025–3036. published online EpubJul 1. [pii]. DOI: 10.1172/JCI6878268782 [PubMed: 23921127]
27. Zaret KS, Grompe M. Generation and regeneration of cells of the liver and pancreas. Science. 2008; 322:1490–1494. published online EpubDec 5. [PubMed: 19056973]
28. Soto-Gutierrez A, Kobayashi N, Rivas-Carrillo JD, Navarro-Alvarez N, Zhao D, Okitsu T, Noguchi H, Basma H, Tabata Y, Chen Y, Tanaka K, Narushima M, Miki A, Ueda T, Jun HS, Yoon JW, Lebkowski J, Tanaka N, Fox IJ. Reversal of mouse hepatic failure using an implanted liver-assist device containing ES cell-derived hepatocytes. Nature biotechnology. 2006; 24:1412–1419. published online EpubNov.
29. Duncan AW, Taylor MH, Hickey RD, Hanlon Newell AE, Lenzi ML, Olson SB, Finegold MJ, Grompe M. The ploidy conveyor of mature hepatocytes as a source of genetic variation. Nature. 2010; 467:707–710. published online EpubOct 7. [PubMed: 20861837]
30. Wang B, Zhao L, Fish M, Logan CY, Nusse R. Self-renewing diploid Axin2(+) cells fuel homeostatic renewal of the liver. Nature. 2015; 524:180–185. published online EpubAug 13. DOI: 10.1038/nature14863 [PubMed: 26245375]
31. Wangensteen KJ, Zhang S, Greenbaum LE, Kaestner KH. A genetic screen reveals Foxa3 and TNFR1 as key regulators of liver repopulation. Genes & development. 2015; 29:904–909. published online EpubMay 1. DOI: 10.1101/gad.258855.115 [PubMed: 25934503]
32. Rosen C, Shezen E, Aronovich A, Klionsky YZ, Yaakov Y, Assayag M, Biton IE, Tal O, Shakhar G, Ben-Hur H, Shneider D, Vaknin Z, Sadan O, Evron S, Freud E, Shoseyov D, Wilschanski M, Berkman N, Fibbe WE, Hagin D, Hillel-Karniel C, Krentsis IM, Bachar-Lustig E, Reisner Y. Preconditioning allows engraftment of mouse and human embryonic lung cells, enabling lung repair in mice. Nature medicine. 2015; 21:869–879. published online EpubAug. DOI: 10.1038/nm.3889
33. Yanger K, Knigin D, Zong Y, Maggs L, Gu G, Akiyama H, Pikarsky E, Stanger BZ. Adult hepatocytes are generated by self-duplication rather than stem cell differentiation. Cell stem cell. 2014; 15:340–349. published online EpubSep 4. DOI: 10.1016/j.stem.2014.06.003 [PubMed: 25130492]
34. Zhu S, Rezvani M, Harbell J, Mattis AN, Wolfe AR, Benet LZ, Willenbring H, Ding S. Mouse liver repopulation with hepatocytes generated from human fibroblasts. Nature. 2014; 508:93–97. published online EpubApr 03. DOI: 10.1038/nature13020 [PubMed: 24572354]
35. Fan F, He Z, Kong LL, Chen Q, Yuan Q, Zhang S, Ye J, Liu H, Sun X, Geng J, Yuan L, Hong L, Xiao C, Zhang W, Sun X, Li Y, Wang P, Huang L, Wu X, Ji Z, Wu Q, Xia NS, Gray NS, Chen L, Yun CH, Deng X, Zhou D. Pharmacological targeting of kinases MST1 and MST2 augments

tissue repair and regeneration. Science translational medicine. 2016; 8:352ra108. published online EpubAug 17. doi: 10.1126/scitranslmed.aaf2304

36. Huang P, He Z, Ji S, Sun H, Xiang D, Liu C, Hu Y, Wang X, Hui L. Induction of functional hepatocyte-like cells from mouse fibroblasts by defined factors. Nature. 2011; 475:386–389. published online EpubMay 11. DOI: 10.1038/nature10116 [PubMed: 21562492]
37. Sekiya S, Suzuki A. Direct conversion of mouse fibroblasts to hepatocyte-like cells by defined factors. Nature. 2011; 475:390–393. published online EpubJun 29. DOI: 10.1038/nature10263 [PubMed: 21716291]
38. Li X, Liu D, Ma Y, Du X, Jing J, Wang L, Xie B, Sun D, Sun S, Jin X, Zhang X, Zhao T, Guan J, Yi Z, Lai W, Zheng P, Huang Z, Chang Y, Chai Z, Xu J, Deng H. Direct Reprogramming of Fibroblasts via a Chemically Induced XEN-like State. Cell stem cell. 2017; published online EpubJun 20. doi: 10.1016/j.stem.2017.05.019
39. Kordes C, Haussinger D. Hepatic stem cell niches. The Journal of clinical investigation. 2013; 123:1874–1880. published online EpubMay. DOI: 10.1172/JCI66027 [PubMed: 23635785]
40. Pardo-Saganta A, Tata PR, Law BM, Saez B, Chow R, Prabhu M, Gridley T, Rajagopal J. Parent stem cells can serve as niches for their daughter cells. Nature. 2015; 523:597–601. published online EpubJul 30. DOI: 10.1038/nature14553 [PubMed: 26147083]
41. Hidalgo A, Chang J, Jang JE, Peired AJ, Chiang EY, Frenette PS. Heterotypic interactions enabled by polarized neutrophil microdomains mediate thromboinflammatory injury. Nature medicine. 2009; 15:384–391. published online EpubApr.
42. Boulter L, Govaere O, Bird TG, Radulescu S, Ramachandran P, Pellicoro A, Ridgway RA, Seo SS, Spee B, Van Rooijen N, Sansom OJ, Iredale JP, Lowell S, Roskams T, Forbes SJ. Macrophage-derived Wnt opposes Notch signaling to specify hepatic progenitor cell fate in chronic liver disease. Nature medicine. 2012; 18:572–579. published online EpubApr. DOI: 10.1038/nm.2667
43. Branchfield K, Nantie L, Verheyden JM, Sui P, Wienhold MD, Sun X. Pulmonary neuroendocrine cells function as airway sensors to control lung immune response. Science. 2016; 351:707–710. published online EpubFeb 12. DOI: 10.1126/science.aad7969 [PubMed: 26743624]
44. Peng T, Frank DB, Kadzik RS, Morley MP, Rathi KS, Wang T, Zhou S, Cheng L, Lu MM, Morrisey EE. Hedgehog actively maintains adult lung quiescence and regulates repair and regeneration. Nature. 2015; 526:578–582. published online EpubOct 22. DOI: 10.1038/nature14984 [PubMed: 26436454]
45. Lechner AJ, Driver IH, Lee J, Conroy CM, Nagle A, Locksley RM, Rock JR. Recruited Monocytes and Type 2 Immunity Promote Lung Regeneration following Pneumonectomy. Cell stem cell. 2017; published online EpubMay 11. doi: 10.1016/j.stem.2017.03.024
46. Paris AJ, Liu Y, Mei J, Dai N, Guo L, Spruce LA, Hudock KM, Brenner JS, Zacharias WJ, Mei HD, Slamowitz AR, Bhamidipati K, Beers MF, Seeholzer SH, Morrisey EE, Worthen GS. Neutrophils promote alveolar epithelial regeneration by enhancing type II pneumocyte proliferation in a model of acid-induced acute lung injury. American journal of physiology Lung cellular and molecular physiology. 2016; 311:L1062–L1075. published online EpubDec 01. DOI: 10.1152/ajplung.00327.2016 [PubMed: 27694472]
47. Lefrancais E, Ortiz-Munoz G, Caudrillier A, Mallavia B, Liu F, Sayah DM, Thornton EE, Headley MB, David T, Coughlin SR, Krummel MF, Leavitt AD, Passegue E, Looney MR. The lung is a site of platelet biogenesis and a reservoir for haematopoietic progenitors. Nature. 2017; 544:105–109. published online EpubApr 06. DOI: 10.1038/nature21706 [PubMed: 28329764]
48. LeCouter J, Moritz DR, Li B, Phillips GL, Liang XH, Gerber HP, Hillan KJ, Ferrara N. Angiogenesis-independent endothelial protection of liver: role of VEGFR-1. Science. 2003; 299:890–893. published online EpubFeb 7. [PubMed: 12574630]
49. Matsumoto K, Yoshitomi H, Rossant J, Zaret KS. Liver organogenesis promoted by endothelial cells prior to vascular function. Science. 2001; 294:559–563. published online EpubOct 19. [PubMed: 11577199]
50. Michalopoulos GK, DeFrances MC. Liver regeneration. Science. 1997; 276:60–66. published online EpubApr 4. [PubMed: 9082986]
51. Wei K, Piecewicz SM, McGinnis LM, Taniguchi CM, Wiegand SJ, Anderson K, Chan CW, Mulligan KX, Kuo D, Yuan J, Vallon M, Morton LC, Lefai E, Simon MC, Maher JJ, Mithieux G,

Rajas F, Annes JP, McGuinness OP, Thurston G, Giaccia AJ, Kuo CJ. A liver Hif-2alpha-Irs2 pathway sensitizes hepatic insulin signaling and is modulated by Vegf inhibition. Nature medicine. 2013; 19:1331–1337. published online EpubOct. DOI: 10.1038/nm.3295

52. Wang L, Wang X, Xie G, Wang L, Hill CK, Deleve LD. Liver sinusoidal endothelial cell progenitor cells promote liver regeneration in rats. The Journal of clinical investigation. 2012; 122:1567–1573. published online EpubApr 2. [PubMed: 22406533]
53. Islam MN, Das SR, Emin MT, Wei M, Sun L, Westphalen K, Rowlands DJ, Quadri SK, Bhattacharya S, Bhattacharya J. Mitochondrial transfer from bone-marrow-derived stromal cells to pulmonary alveoli protects against acute lung injury. Nature medicine. 2012; 18:759–765. published online EpubMay.
54. Beers MF, Morrisey EE. The three R's of lung health and disease: repair, remodeling, and regeneration. The Journal of clinical investigation. 2011; 121:2065–2073. published online EpubJun 1. [PubMed: 21633173]
55. Ding BS, Liu CH, Sun Y, Chen Y, Swendeman SL, Jung B, Chavez D, Cao Z, Christoffersen C, Nielsen LB, Schwab SR, Rafii S, Hla T. HDL activation of endothelial sphingosine-1-phosphate receptor-1 (S1P1) promotes regeneration and suppresses fibrosis in the liver. JCI insight. 2016; 1:e87058. published online EpubDec 22. doi: 10.1172/jci.insight.87058 [PubMed: 28018969]
56. Hecker L, Vittal R, Jones T, Jagirdar R, Luckhardt TR, Horowitz JC, Pennathur S, Martinez FJ, Thannickal VJ. NADPH oxidase-4 mediates myofibroblast activation and fibrogenic responses to lung injury. Nature medicine. 2009; 15:1077–1081. published online EpubSep.
57. Henderson NC, Arnold TD, Katamura Y, Giacomini MM, Rodriguez JD, McCarty JH, Pellicoro A, Raschperger E, Betsholtz C, Ruminski PG, Griggs DW, Prinsen MJ, Maher JJ, Iredale JP, Lacy-Hulbert A, Adams RH, Sheppard D. Targeting of alphav integrin identifies a core molecular pathway that regulates fibrosis in several organs. Nature medicine. 2013; 19:1617–1624. published online EpubDec.
58. Noble PW, Barkauskas CE, Jiang D. Pulmonary fibrosis: patterns and perpetrators. The Journal of clinical investigation. 2012; 122:2756–2762. published online EpubAug 1. [PubMed: 22850886]
59. Seki E, De Minicis S, Osterreicher CH, Kluwe J, Osawa Y, Brenner DA, Schwabe RF. TLR4 enhances TGF-beta signaling and hepatic fibrosis. Nature medicine. 2007; 13:1324–1332. published online EpubNov.
60. Zeisberg EM, Tarnavski O, Zeisberg M, Dorfman AL, McMullen JR, Gustafsson E, Chandraker A, Yuan X, Pu WT, Roberts AB, Neilson EG, Sayegh MH, Izumo S, Kalluri R. Endothelial-to-mesenchymal transition contributes to cardiac fibrosis. Nature medicine. 2007; 13:952–961. published online EpubAug.
61. Pellicoro A, Ramachandran P, Iredale JP, Fallowfield JA. Liver fibrosis and repair: immune regulation of wound healing in a solid organ. Nature reviews. 2014; 14:181–194. published online EpubMar. DOI: 10.1038/nri3623
62. Herazo-Maya JD, Noth I, Duncan SR, Kim S, Ma SF, Tseng GC, Feingold E, Juan-Guardela BM, Richards TJ, Lussier Y, Huang Y, Vij R, Lindell KO, Xue J, Gibson KF, Shapiro SD, Garcia JG, Kaminski N. Peripheral blood mononuclear cell gene expression profiles predict poor outcome in idiopathic pulmonary fibrosis. Science translational medicine. 2013; 5:205ra136. published online EpubOct 2. doi: 10.1126/scitranslmed.3005964
63. Zhou Y, Peng H, Sun H, Peng X, Tang C, Gan Y, Chen X, Mathur A, Hu B, Slade MD, Montgomery RR, Shaw AC, Homer RJ, White ES, Lee CM, Moore MW, Gulati M, Lee CG, Elias JA, Herzog EL. Chitinase 3-like 1 suppresses injury and promotes fibroproliferative responses in Mammalian lung fibrosis. Science translational medicine. 2014; 6:240ra276. published online EpubJun 11. doi: 10.1126/scitranslmed.3007096
64. Ramachandran P, Iredale JP. Macrophages: central regulators of hepatic fibrogenesis and fibrosis resolution. Journal of hepatology. 2012; 56:1417–1419. published online EpubJun. DOI: 10.1016/j.jhep.2011.10.026 [PubMed: 22314426]
65. Coon TA, McKelvey AC, Lear T, Rajbhandari S, Dunn SR, Connelly W, Zhao JY, Han S, Liu Y, Weathington NM, McVerry BJ, Zhang Y, Chen BB. The proinflammatory role of HECTD2 in innate immunity and experimental lung injury. Science translational medicine. 2015; 7:295ra109. published online EpubJul 8. doi: 10.1126/scitranslmed.aab3881

66. Zou C, Li J, Xiong S, Chen Y, Wu Q, Li X, Weathington NM, Han S, Snavely C, Chen BB, Mallampalli RK. Mortality factor 4 like 1 protein mediates epithelial cell death in a mouse model of pneumonia. Science translational medicine. 2015; 7:311ra171. published online EpubOct 28. doi: 10.1126/scitranslmed.aac7793

67. Tager AM, LaCamera P, Shea BS, Campanella GS, Selman M, Zhao Z, Polosukhin V, Wain J, Karimi-Shah BA, Kim ND, Hart WK, Pardo A, Blackwell TS, Xu Y, Chun J, Luster AD. The lysophosphatidic acid receptor LPA1 links pulmonary fibrosis to lung injury by mediating fibroblast recruitment and vascular leak. Nature medicine. 2008; 14:45–54. published online EpubJan. DOI: 10.1038/nm1685

68. El Agha E, Moiseenko A, Kheirollahi V, De Langhe S, Crnkovic S, Kwapiszewska G, Kosanovic D, Schwind F, Schermuly RT, Henneke I, MacKenzie B, Quantius J, Herold S, Ntokou A, Ahlbrecht K, Morty RE, Gunther A, Seeger W, Bellusci S. Two-Way Conversion between Lipogenic and Myogenic Fibroblastic Phenotypes Marks the Progression and Resolution of Lung Fibrosis. Cell stem cell. 2017; 20:261–273 e263. published online EpubFeb 02. DOI: 10.1016/j.stem.2016.10.004 [PubMed: 27867035]

69. Yin C, Evason KJ, Asahina K, Stainier DY. Hepatic stellate cells in liver development, regeneration, and cancer. The Journal of clinical investigation. 2013; 123:1902–1910. published online EpubMay. DOI: 10.1172/JCI66369 [PubMed: 23635788]

70. Lee JH, Bhang DH, Beede A, Huang TL, Stripp BR, Bloch KD, Wagers AJ, Tseng YH, Ryeom S, Kim CF. Lung Stem Cell Differentiation in Mice Directed by Endothelial Cells via a BMP4-NFATc1-Thrombospondin-1 Axis. Cell. 2014; 156:440–455. published online EpubJan 30. [PubMed: 24485453]

71. Petrache I, Natarajan V, Zhen L, Medler TR, Richter AT, Cho C, Hubbard WC, Berdyshev EV, Tuder RM. Ceramide upregulation causes pulmonary cell apoptosis and emphysema-like disease in mice. Nature medicine. 2005; 11:491–498. published online EpubMay.

72. Cai Y, Bolte C, Le T, Goda C, Xu Y, Kalin TV, Kalinichenko VV. FOXF1 maintains endothelial barrier function and prevents edema after lung injury. Science signaling. 2016; 9:ra40. published online EpubApr 19. doi: 10.1126/scisignal.aad1899 [PubMed: 27095594]

73. Mirza MK, Sun Y, Zhao YD, Potula HH, Frey RS, Vogel SM, Malik AB, Zhao YY. FoxM1 regulates re-annealing of endothelial adherens junctions through transcriptional control of beta-catenin expression. The Journal of experimental medicine. 2010; 207:1675–1685. published online EpubAug 02. DOI: 10.1084/jem.20091857 [PubMed: 20660612]

74. Carmeliet P, Jain RK. Molecular mechanisms and clinical applications of angiogenesis. Nature. 2011; 473:298–307. published online EpubMay 19. [PubMed: 21593862]

75. Rafii S, Butler JM, Ding BS. Angiocrine functions of organ-specific endothelial cells. Nature. 2016; 529:316–325. published online EpubJan 21. DOI: 10.1038/nature17040 [PubMed: 26791722]

76. Hecker L, Logsdon NJ, Kurundkar D, Kurundkar A, Bernard K, Hock T, Meldrum E, Sanders YY, Thannickal VJ. Reversal of persistent fibrosis in aging by targeting Nox4-Nrf2 redox imbalance. Science translational medicine. 2014; 6:231ra247. published online EpubApr 09. doi: 10.1126/scitranslmed.3008182

77. Moon JS, Nakahira K, Chung KP, DeNicola GM, Koo MJ, Pabon MA, Rooney KT, Yoon JH, Ryter SW, Stout-Delgado H, Choi AM. NOX4-dependent fatty acid oxidation promotes NLRP3 inflammasome activation in macrophages. Nature medicine. 2016; 22:1002–1012. published online EpubSep. DOI: 10.1038/nm.4153

78. Nishikawa T, Bell A, Brooks JM, Setoyama K, Melis M, Han B, Fukumitsu K, Handa K, Tian J, Kaestner KH, Vodovotz Y, Locker J, Soto-Gutierrez A, Fox IJ. Resetting the transcription factor network reverses terminal chronic hepatic failure. The Journal of clinical investigation. 2015; 125:1533–1544. published online EpubApr. [PubMed: 25774505]

79. Ding BS, Nolan DJ, Guo P, Babazadeh AO, Cao Z, Rosenwaks Z, Crystal RG, Simons M, Sato TN, Worgall S, Shido K, Rabbany SY, Rafii S. Endothelial-derived angiocrine signals induce and sustain regenerative lung alveolarization. Cell. 2011; 147:539–553. published online EpubOct 28. [PubMed: 22036563]

80. Ding BS, Nolan DJ, Butler JM, James D, Babazadeh AO, Rosenwaks Z, Mittal V, Kobayashi H, Shido K, Lyden D, Sato TN, Rabbany SY, Rafii S. Inductive angiocrine signals from sinusoidal

endothelium are required for liver regeneration. Nature. 2010; 468:310–315. published online EpubNov 11. DOI: 10.1038/nature09493 [PubMed: 21068842]

81. Bhushan B, Walesky C, Manley M, Gallagher T, Borude P, Edwards G, Monga SP, Apte U. Pro-regenerative signaling after acetaminophen-induced acute liver injury in mice identified using a novel incremental dose model. The American journal of pathology. 2014; 184:3013–3025. published online EpubNov. S0002-9440(14)00437-4 [pii]. DOI: 10.1016/j.ajpath.2014.07.019 [PubMed: 25193591]
82. Ding J, Yannam GR, Roy-Chowdhury N, Hidvegi T, Basma H, Rennard SI, Wong RJ, Avsar Y, Guha C, Perlmutter DH, Fox IJ, Roy-Chowdhury J. Spontaneous hepatic repopulation in transgenic mice expressing mutant human alpha1-antitrypsin by wild-type donor hepatocytes. The Journal of clinical investigation. 2011; 121:1930–1934. published online EpubMay. DOI: 10.1172/JCI45260 [PubMed: 21505264]
83. Fafalios A, Ma J, Tan X, Stoops J, Luo J, Defrances MC, Zarnegar R. A hepatocyte growth factor receptor (Met)-insulin receptor hybrid governs hepatic glucose metabolism. Nature medicine. 2011; 17:1577–1584. published online EpubNov 13. DOI: 10.1038/nm.2531
84. Wang Y, Nakayama M, Pitulescu ME, Schmidt TS, Bochenek ML, Sakakibara A, Adams S, Davy A, Deutsch U, Luthi U, Barberis A, Benjamin LE, Makinen T, Nobes CD, Adams RH. Ephrin-B2 controls VEGF-induced angiogenesis and lymphangiogenesis. Nature. 2010; 465:483–486. published online EpubMay 27. [PubMed: 20445537]
85. Martinez-Palacian A, del Castillo G, Suarez-Causado A, Garcia-Alvaro M, de Morena-Frutos D, Fernandez M, Roncero C, Fabregat I, Herrera B, Sanchez A. Mouse hepatic oval cells require Met-dependent PI3K to impair TGF-beta-induced oxidative stress and apoptosis. PloS one. 2013; 8:e53108.doi: 10.1371/journal.pone.0053108 [PubMed: 23301029]
86. Fan-Minogue H, Cao Z, Paulmurugan R, Chan CT, Massoud TF, Felsher DW, Gambhir SS. Noninvasive molecular imaging of c-Myc activation in living mice. Proceedings of the National Academy of Sciences of the United States of America. 2010; 107:15892–15897. published online EpubSep 7. DOI: 10.1073/pnas.1007443107 [PubMed: 20713710]
87. Kozower BD, Christofidou-Solomidou M, Sweitzer TD, Muro S, Buerk DG, Solomides CC, Albelda SM, Patterson GA, Muzykantov VR. Immunotargeting of catalase to the pulmonary endothelium alleviates oxidative stress and reduces acute lung transplantation injury. Nature biotechnology. 2003; 21:392–398. published online EpubApr.
88. Oh P, Borgstrom P, Witkiewicz H, Li Y, Borgstrom BJ, Chrastina A, Iwata K, Zinn KR, Baldwin R, Testa JE, Schnitzer JE. Live dynamic imaging of caveolae pumping targeted antibody rapidly and specifically across endothelium in the lung. Nature biotechnology. 2007; 25:327–337. published online EpubMar.
89. Reynolds PN, Nicklin SA, Kaliberova L, Boatman BG, Grizzle WE, Balyasnikova IV, Baker AH, Danilov SM, Curiel DT. Combined transductional and transcriptional targeting improves the specificity of transgene expression in vivo. Nature biotechnology. 2001; 19:838–842. published online EpubSep.
90. Morizono K, Xie Y, Ringpis GE, Johnson M, Nassanian H, Lee B, Wu L, Chen IS. Lentiviral vector retargeting to P-glycoprotein on metastatic melanoma through intravenous injection. Nature medicine. 2005; 11:346–352. published online EpubMar.
91. Yamamoto H, Yun EJ, Gerber HP, Ferrara N, Whitsett JA, Vu TH. Epithelial-vascular cross talk mediated by VEGF-A and HGF signaling directs primary septae formation during distal lung morphogenesis. Developmental biology. 2007; 308:44–53. published online EpubAug 1. [PubMed: 17583691]
92. Matsumoto K, Nakamura T. Hepatocyte growth factor: molecular structure and implications for a central role in liver regeneration. J Gastroenterol Hepatol. 1991; 6:509–519. published online EpubSep–Oct. [PubMed: 1834243]
93. Huh CG, Factor VM, Sanchez A, Uchida K, Conner EA, Thorgeirsson SS. Hepatocyte growth factor/c-met signaling pathway is required for efficient liver regeneration and repair. Proceedings of the National Academy of Sciences of the United States of America. 2004; 101:4477–4482. published online EpubMar 30. [PubMed: 15070743]
94. Awuah PK, Nejak-Bowen KN, Monga SP. Role and regulation of PDGFRalpha signaling in liver development and regeneration. The American journal of pathology. 2013; 182:1648–1658.

published online EpubMay. S0002-9440(13)00135-1 [pii]. DOI: 10.1016/j.ajpath.2013.01.047 [PubMed: 23529017]

95. Sancho P, Mainez J, Crosas-Molist E, Roncero C, Fernandez-Rodriguez CM, Pinedo F, Huber H, Eferl R, Mikulits W, Fabregat I. NADPH oxidase NOX4 mediates stellate cell activation and hepatocyte cell death during liver fibrosis development. PloS one. 2012; 7:e45285.doi: 10.1371/journal.pone.0045285 [PubMed: 23049784]
96. Cao Z, Ding BS, Guo P, Lee SB, Butler JM, Casey SC, Simons M, Tam W, Felsher DW, Shido K, Rafii A, Scandura JM, Rafii S. Angiocrine factors deployed by tumor vascular niche induce B cell lymphoma invasiveness and chemoresistance. Cancer cell. 2014; 25:350–365. published online EpubMar 17. [PubMed: 24651014]
97. Cao Z, Scandura JM, Inghirami GG, Shido K, Ding BS, Rafii S. Molecular Checkpoint Decisions Made by Subverted Vascular Niche Transform Indolent Tumor Cells into Chemoresistant Cancer Stem Cells. Cancer cell. 2017; 31:110–126. published online EpubJan 09. DOI: 10.1016/j.ccell.2016.11.010 [PubMed: 27989801]
98. Rafii S, Cao Z, Lis R, Siempos, Chavez D, Shido K, Rabbany SY, Ding BS. Platelet-derived SDF-1 primes the pulmonary capillary vascular niche to drive lung alveolar regeneration. Nature cell biology. 2015; 17:123–136. published online EpubFeb. [PubMed: 25621952]
99. Hoot KE, Oka M, Han G, Bottinger E, Zhang Q, Wang XJ. HGF upregulation contributes to angiogenesis in mice with keratinocyte-specific Smad2 deletion. The Journal of clinical investigation. 2010; 120:3606–3616. published online EpubOct 1. [PubMed: 20852387]
100. Degryse AL, Tanjore H, Xu XC, Polosukhin VV, Jones BR, McMahon FB, Gleaves LA, Blackwell TS, Lawson WE. Repetitive intratracheal bleomycin models several features of idiopathic pulmonary fibrosis. American journal of physiology Lung cellular and molecular physiology. 2010; 299:L442–452. published online EpubOct. [PubMed: 20562227]

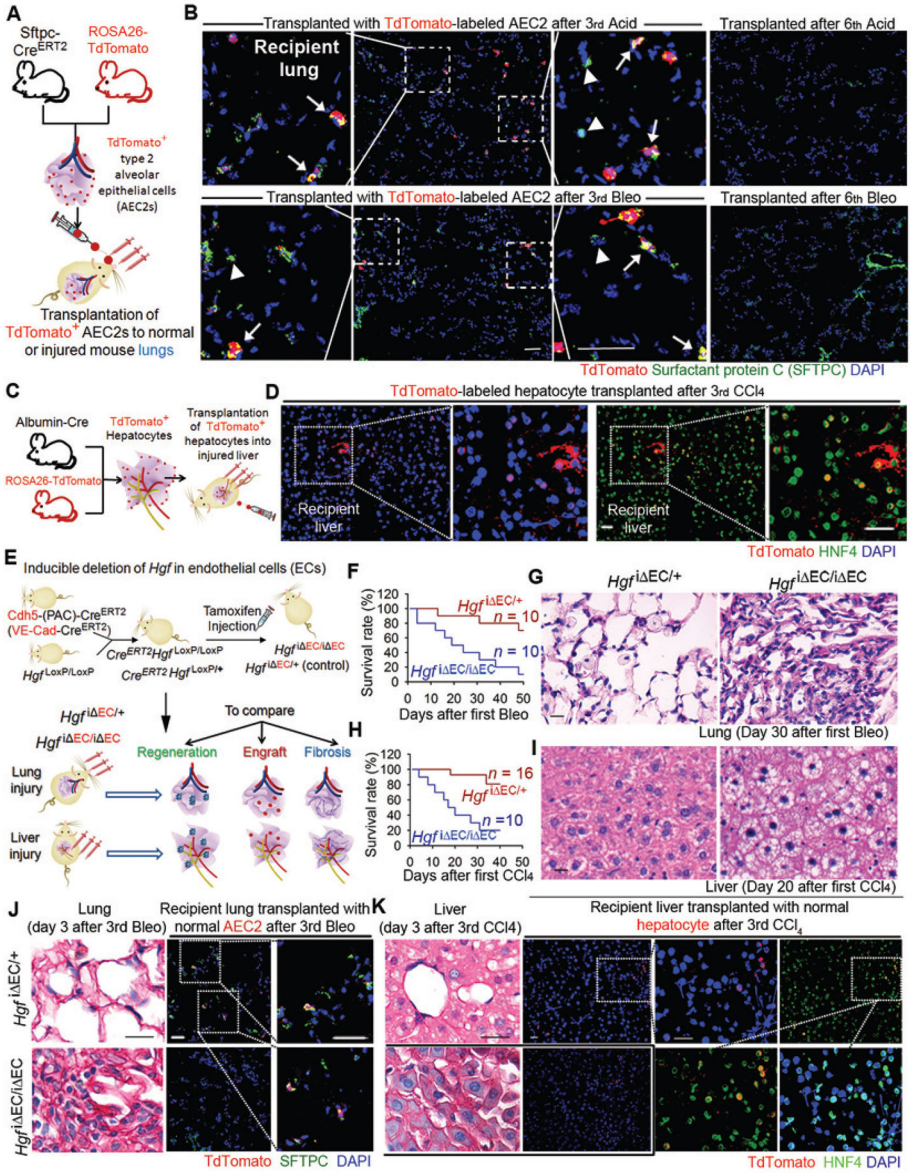

Fig. 1. EC-produced HGF promotes reconstitution of transplanted parenchymal cells in the injured lung and liver in mice

(**A**) Schema illustrating the strategy to test incorporation of transplanted alveolar epithelial progenitor in normal and injured lungs. TdTomato-expressing AEC2s (red) were instilled into recipient lungs via trachea. To induce lung repair, mice were subjected to multiple intratracheal injections of Acid or Bleo.

(B) Immunostaining of SFTPC performed to visualize endogenous ($TdTomato^{-}SFTPC^{+}$, indicated by arrow head in inset) and grafted ($TdTomato^{+}SFTPC^{+}$, labeled with arrow in inset) AEC2s in mice after three Bleo or Acid injections. Result of AEC2 transplantation in normal mouse lungs is shown in fig. S1A.

(**C**) Approach to examine the incorporation of hepatocytes in normal and injured mouse livers. Hepatocytes were transplanted to recipient mice via intrasplenic injection of

TdTomato$^+$ hepatocytes, and sections were co-stained with hepatocyte marker hepatic nuclear factor 4α (HNF4).

(**D**) Immunostaining showing incorporation of transplanted HNF4$^+$TdTomato$^+$ hepatocytes in the liver after three injections of CCl_4. Incorporation of hepatocytes transplanted after 8th CCl_4 and data showing hepatocytes transplanted into normal mice are presented in fig. S1B, C.

(E) Schema illustrating the approach to test organ regeneration, fibrosis, and incorporation of parenchymal cells in mice with EC-specific deletion of *Hgf* (*Hgf*$^{i\Delta EC/i\Delta EC}$). *Hgf*$^{i\Delta EC/i\Delta EC}$ and control *Hgf*$^{i\Delta EC/+}$ mice were subjected to lung and liver injury and transplanted with TdTomato$^+$ AEC2s or hepatocytes. Regeneration, fibrosis, and incorporation of injected parenchymal cells (engraftment) were compared between *Hgf*$^{i\Delta EC/i\Delta EC}$ and control mice.

(**F**) Survival rate of *Hgf*$^{i\Delta EC/i\Delta EC}$ and *Hgf*$^{i\Delta EC/+}$ mice after Bleo injection every 12 days.

(**G**) Sirius red staining of lung tissue from mice in (F).

(**H**) Survival rate of *Hgf*$^{i\Delta EC/i\Delta EC}$ and *Hgf*$^{i\Delta EC/+}$ mice after CCl_4 injection every 3 days.

(**I**) Sirius red staining of liver tissue from mice in (H).

(**J**) Sirius red staining depicting collagen deposition, and immunostaining illustrating transplanted AEC2s (red) in the injured mouse lungs.

(K) Sirius red staining and immunostaining showing transplanted hepatocytes (red) in the injured mouse livers. Five mice per group were analyzed for qualitative staining experiments. Scale bars, 50 μm.

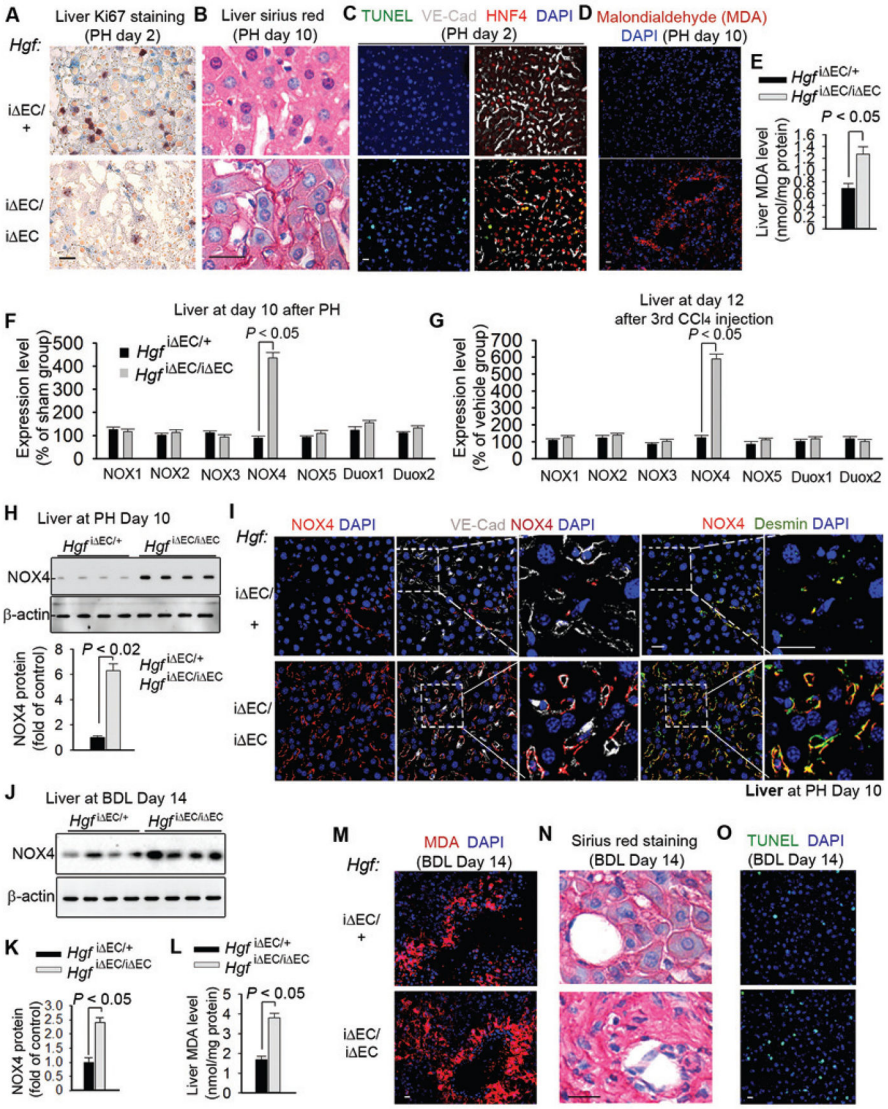

Figure 2. HGF from ECs reduces NADPH Oxidase 4 (NOX4) expression in perivascular fibroblasts to bypass fibrosis during liver regeneration

(**A–E**) Liver sections from *Hgf*$^{i\Delta EC/+}$ (control) and *Hgf*$^{i\Delta EC/i\Delta EC}$ mice after partial hepatectomy (PH) showing (A) Ki67 staining for proliferation, (B) Sirius red staining for collagen, (C) immunostaining for TUNEL, VE-cadherin, and HNF4, (D) malondialdehyde (MDA) staining for peroxide formation, and (E) MDA quantity. $n = 7$ *Hgf*$^{i\Delta EC/i\Delta EC}$ mice and 8 control mice.

(**F–G**) mRNA expression of NOX family members in liver tissue from *Hgf*$^{i\Delta EC/i\Delta EC}$ and control mice (F) 10 days after PH and (G) 12 days after CCl_4 injections; $n = 10$ control and 11 *Hgf*$^{i\Delta EC/i\Delta EC}$ mice in PH group and 12 mice in CCl_4 group.

(**H**) Western blot and quantification of NOX4 protein in liver tissue from *Hgf*$^{i\Delta EC/i\Delta EC}$ and control mice after PH. $n = 8$ mice per group.

(**I**) Immunostaining of fibroblast marker desmin, VE-cadherin, and NOX4 in liver sections from mice 10 days after PH. Insets show co-localization of NOX4 with desmin^{+} fibroblasts adjacent to VE-cadherin^{+} liver ECs.

(**J–K**) Western blot and quantification of NOX4 protein in liver tissue from *Hgf*$^{i\Delta EC/i\Delta EC}$ and *Hgf*$^{i\Delta EC/+}$ (control) mice at day 14 after BDL; $n = 8$ mice per group.

(**L–M**) Quantity (L) and immunostaining (M) of MDA in liver tissue from *Hgf*$^{i\Delta EC/i\Delta EC}$ and controls. n = 10 *Hgf*$^{i\Delta EC/i\Delta EC}$ mice and 12 *Hgf*$^{i\Delta EC/+}$ mice.

(**N–O**) Sirius red (N) and TUNEL (O) stainings of liver sections from (L); Statistical difference between two experimental groups was determined by two tailed t-test. Scale bars, 50 μm.

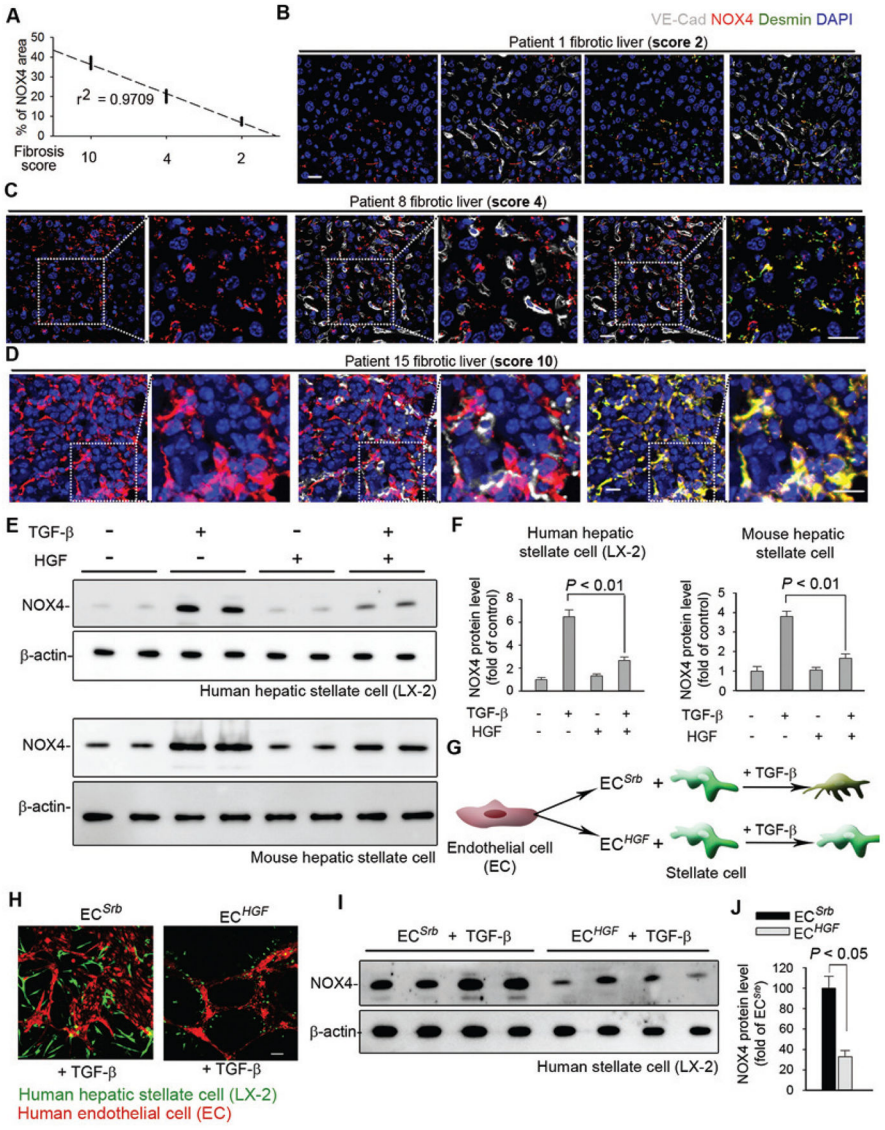

Figure 3. EC-expressed HGF abrogates pro-fibrotic NOX4 induction in human perivascular fibroblasts

(**A**) Correlation between expression of perivascular NOX4 and fibrosis score in individual human patients. Fibrosis score at 2, 4, or 10 was used, with a higher score denoting more severe fibrosis and larger fibrotic area in the observed slide. Each dot in the plot represents individual patient.

(B–D) Representative human liver section immunostaining images from (A). Insets show higher magnification.

(E–F) Western blot and quantification of NOX4 protein in human LX-2 cells and mouse stellate cells treated with 20 ng/ml TGF-β ± 40 ng/ml HGF. Representative blot image is shown in (E), and each lane represents one tested biological sample. $n = 6$ samples for each group. Statistical difference was determined by one-way analysis of variance (ANOVA) followed by Tukey's test as post hoc analysis.

(**G–H**) Representative immunofluorescence image of LX-2 cells cultured with human ECs on Matrigel.
(**I–J**) Western blot and quantification of NOX4 protein in LX-2 cells incubated with human ECs. $n = 6$ samples per group. Statistical difference between experimental groups was calculated by two tailed t-test. Scale bars, 50 μm.

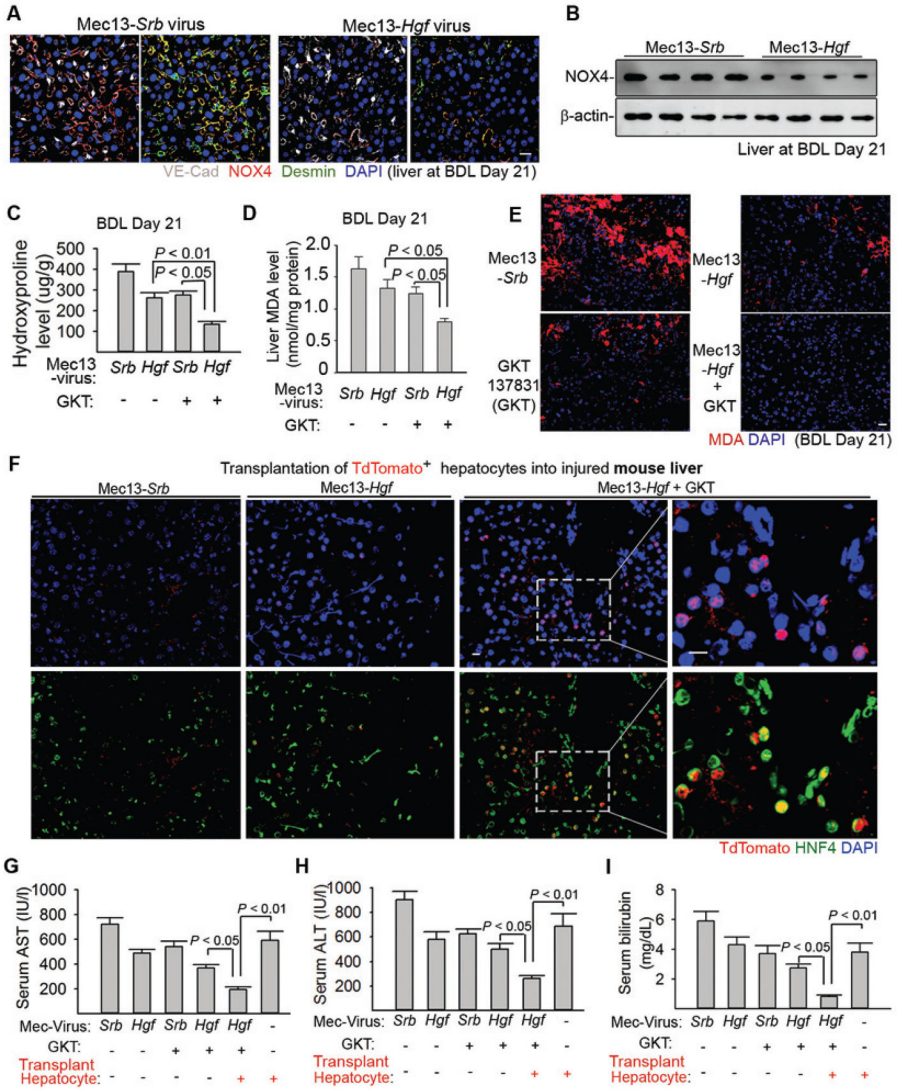

Figure 4. Expression of HGF in liver ECs cooperates with NOX4 inhibition to enhance engraftment of regenerative hepatocytes

(**A–B**) Immunostaining (A) and Western blot (B) of NOX4 protein in the injured liver after injection of pseudotyped virus (90). Antibody Mec13.3 recognizing CD31 was conjugated with virus expressing *Hgf* (Mec13-*Hgf*) or scrambled sequence (Mec13-*Srb*). Virus was injected into the portal circulation. $n = 8$ mice in Mec13-*Hgf* group and 10 mice in Mec13-*Srb* group.

(**C–E**) Liver hydroxyproline and MDA amounts in injured mice treated with Mec13-*Hgf*, NOX4 inhibitor GKT137831 (GKT), or coinjection of Mec13-*Hgf* and GKT (Mec13-*Hgf* + GKT). n = 8, 10, 10, 9 animals in individual groups from left to right in panel C and D. Statistical analysis was performed with one-way ANOVA followed by Tukey's test.

(**F**) Incorporation of transplanted TdTomato$^+$ hepatocytes in the liver tissue of mice 21 days after BDL.

(**G–I**) Serum concentrations of Aspartate aminotransferase (AST) (G), Alanine aminotransferase (ALT) (H), and bilirubin (I) in indicated mouse groups after BDL. n = 12,

16, 14, 16, 15, 12 animals in individual groups from left to right in panel G, H, and I. Statistical difference was deteremined by one-way ANOVA followed by Tukey's test. Scale bars, 50 μm.

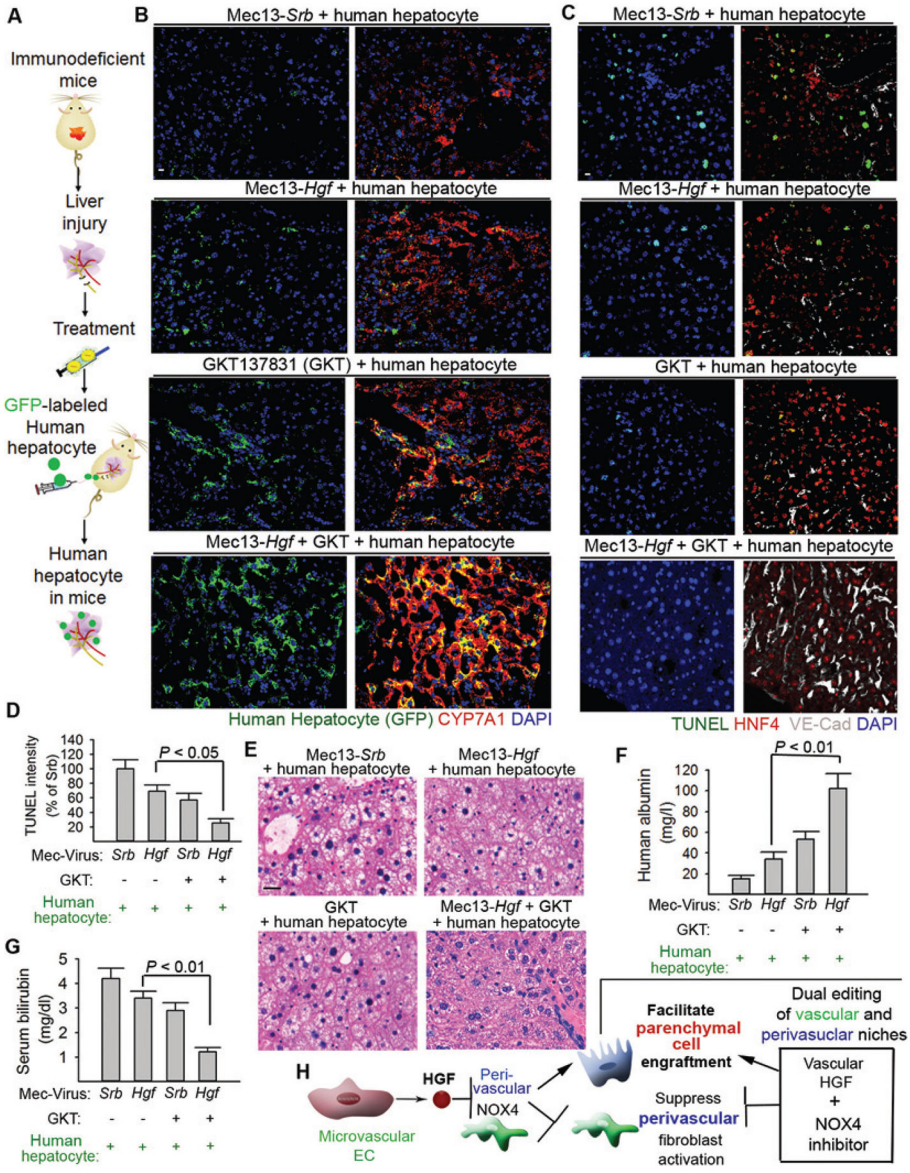

Figure 5. Dual editing of endothelial and perivascular cells promotes incorporation of regenerative human hepatocytes in the liver

(**A**) Schema depicting the strategy to transplant human hepatocytes into NCG mice.

(**B**) Distribution of grafted GFP$^+$ human hepatocytes in the recipient mouse liver after indicated treatments. GFP was co-stained with cholesterol 7 alpha-hydroxylase (CYP7A1) in the liver sections from recipient injured mice.

(**C, D**) Cell apoptosis in NCG mice with indicated treatments and transplanted with hepatocytes. TUNEL was co-stained with HNF4 and VE-cadherin. $n = 5$ mice per group.

(**E–G**) Hepatic pathology and quantity of serum human albumin and bilirubin in recipient mice after BDL. $n = 5$ mice per group.

(**H**) Dual editing of vascular and perivascular niches by endothelial *Hgf* gene delivery and NOX4 inhibition facilitates parenchymal cell engraftment and promotes liver repair.

Statistical analysis in Figure 5 was carried out with one-way ANOVA followed by Tukey's test as post hoc analysis. Scale bars, 50 um.

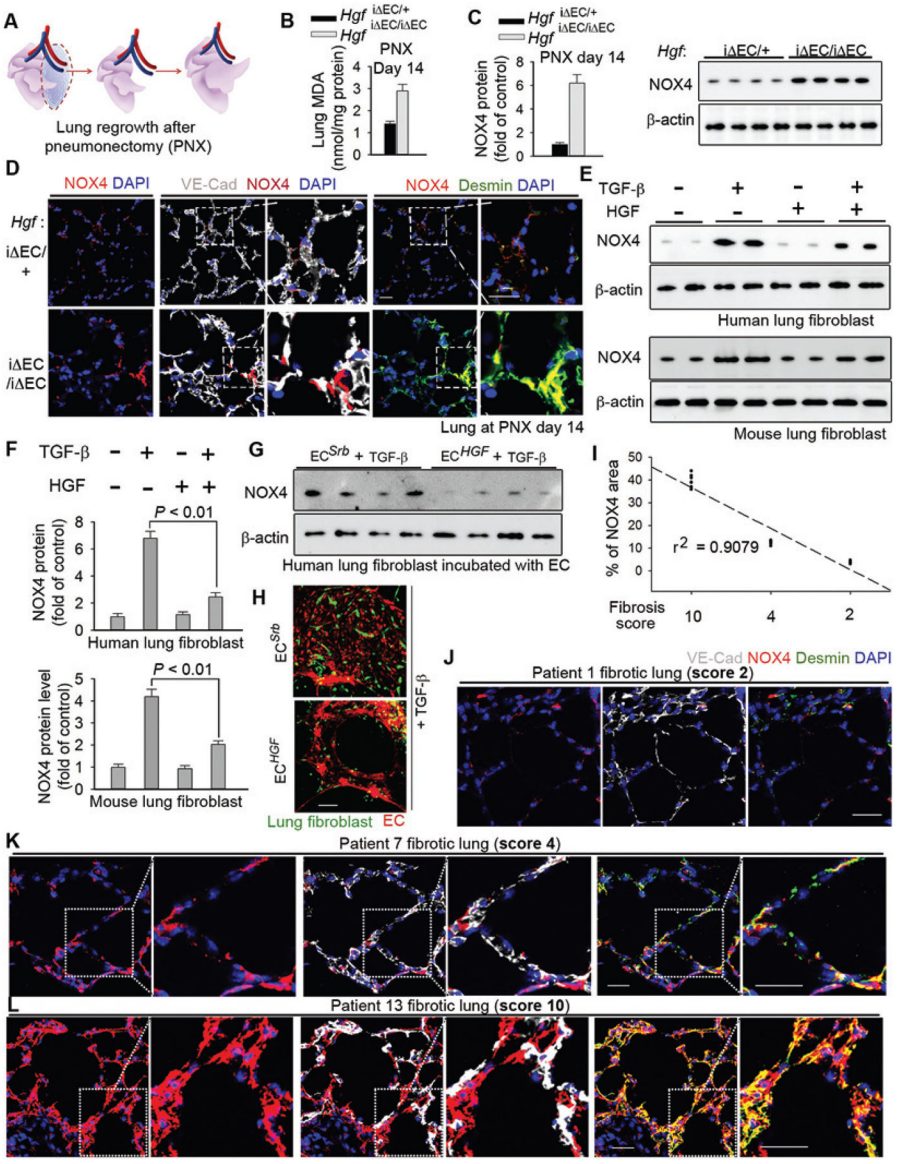

Figure 6. EC-expressed HGF stimulates lung alveolar regeneration and resolves fibrosis

(A) Schema illustrating the strategy to test lung alveolar regrowth after pneumonectomy (PNX).

(B–D) Lung MDA quantity (B), Western blot and quantification (C) and immunostaining (D) of NOX4 protein the lung of *Hgf*$^{i\Delta EC/i\Delta EC}$ and control mice after PNX. $n = 10$ *Hgf*$^{i\Delta EC/i\Delta EC}$ and 16 controls. Insets show the distribution of NOX4 protein in the lungs. Statistical difference between experimental groups was assessed by two tailed t-test.

(E–F) Western blot (E) and quantification (F) of NOX4 protein in human and mouse lung fibroblasts treated with 20 ng/ml TGF-β ± 40 ng/ml HGF. $n = 6$ samples per group. Statistical difference was determined by one-way ANOVA followed by Tukey's test.

(**G**) Western blot of NOX4 protein in human lung fibroblasts incubated with EC^{HGF} or EC^{Srb}.

(**H**) Representative immunofluorescence image of human lung fibroblasts (green) co-cultured with human EC^{HGF} or EC^{Srb} (red) and treated with 10 ng/ml TGF-β.
(I) Correlation between perivascular NOX4 protein quantity and lung fibrosis score in human patients. Each dot in the plot represents data from individual patient.
(J–L) Representative immunostaining image of samples from (I). Insets show the higher magnification. Sale bars, 50 μm.

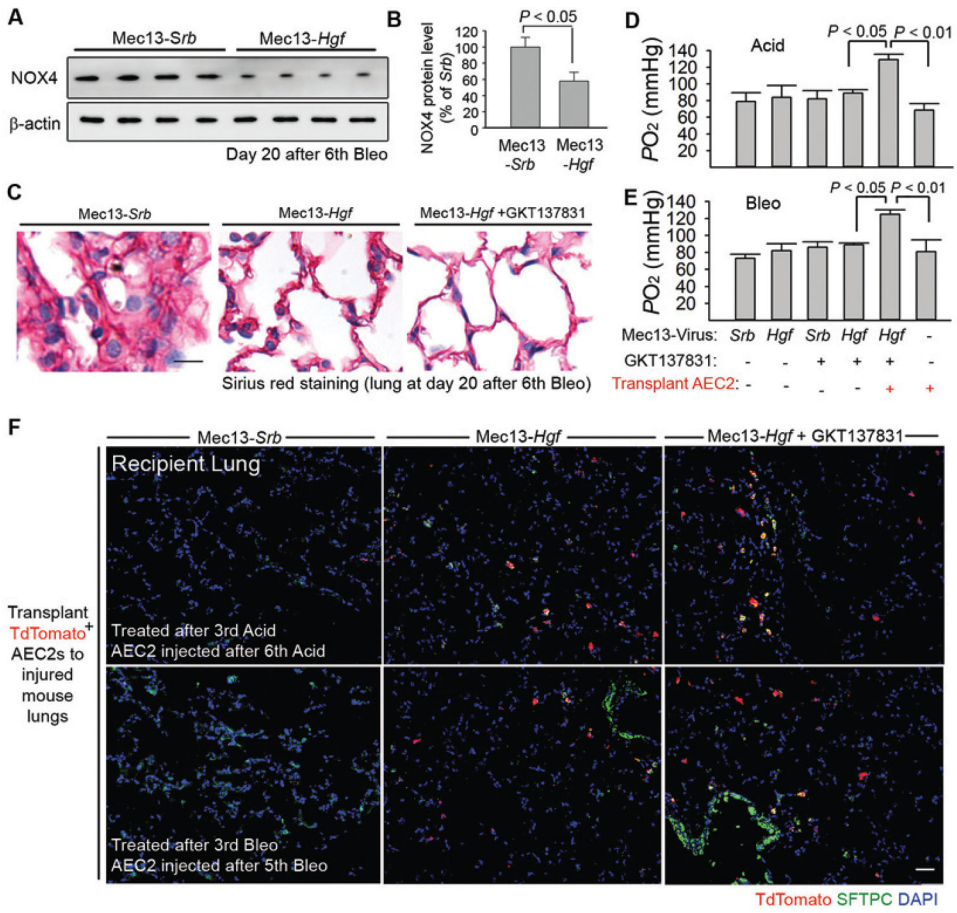

Figure 7. Dual editing of vascular and perivascular niches facilitates incorporation of AEC2s, stimulating fibrosis-free lung repair

(**A–B**) Western blot (A) and quantification (B) of NOX4 protein amount in mouse lungs after Bleo injection and Mec13-*Hgf* or Mec13-*Srb* treatment. $n = 8$ mice per group. Statistical difference between two experimental groups was determined by two tailed t-test.

(**C**) Sirius red staining of lung sections from mice injected with Bleo and treated with Mec13-*Srb*, Mec13-*Hgf*, GKT, or Mec13-*Hgf* + GKT.

(**D, E**) Blood oxygenation in Bleo or Acid-injured mice after treatment of Mec13-*Srb*, Mec13-*Hgf*, GKT, or Mec13-*Hgf* + GKT. AEC2s were transplanted to depicted groups. $n =$ 9, 7, 11, 8, 9, 7 animals in individual groups from left to right in panel D. $n = 10, 8, 9, 7, 8, 8$ mice in individual groups from left to right shown in panel E. Statistical analysis was carried out with one-way ANOVA followed by Tukey's test.

(F) Localization of transplanted TdTomato$^+$ AEC2s (red) in lung tissues from indicated mouse groups. Five mice per group were assessed for qualitative staining analysis. Scale bars, 50 μm.

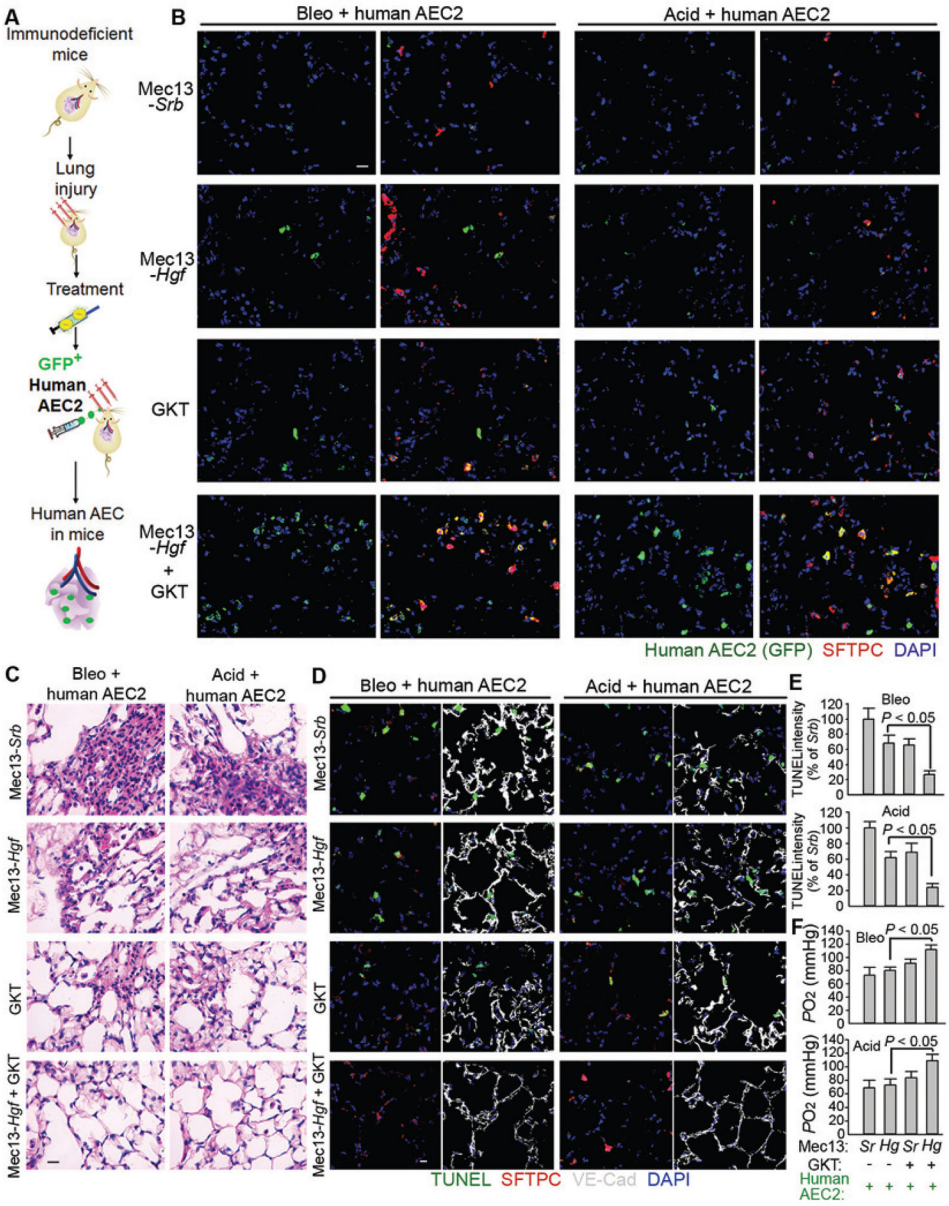

Figure 8. Reconstitution of regenerative human AEC2s in the injured lungs following treatment with Mec13-*Hgf* and GKT

(**A**) Schema describing the approach to graft human AEC2s into NCG mice. Bleo or Acid-injured NCG mice were treated with Mec13-*Srb*, Mec13-*Hgf*, GKT, or Mec13-*Hgf* + GKT and transplanted with human AEC2s.

(**B**) Localization of transplanted GFP$^+$ human AEC2s in the injured lungs from indicated mouse groups. GFP was co-stained with SFTPC. Four mice per group were analyzed in qualitative staining analysis.

(**C–D**) Histological and cell apoptosis analysis of lung sections of mice with indicated injury and treatments.

(**E–F**) Quantification of lung cell apoptosis and blood oxygenation in the injured mice with described treatments. Sr: Mec13-*Srb*; Hg: Mec13-*Hgf*. $n = 5$ mice in all groups except

Mec13-*Srb* group transplanted with AEC2s (Sr group; $n = 4$). Statistical analysis in Figure 8 was performed with one-way ANOVA followed by Tukey's test as post hoc analysis. Scale bars, 50 μm.